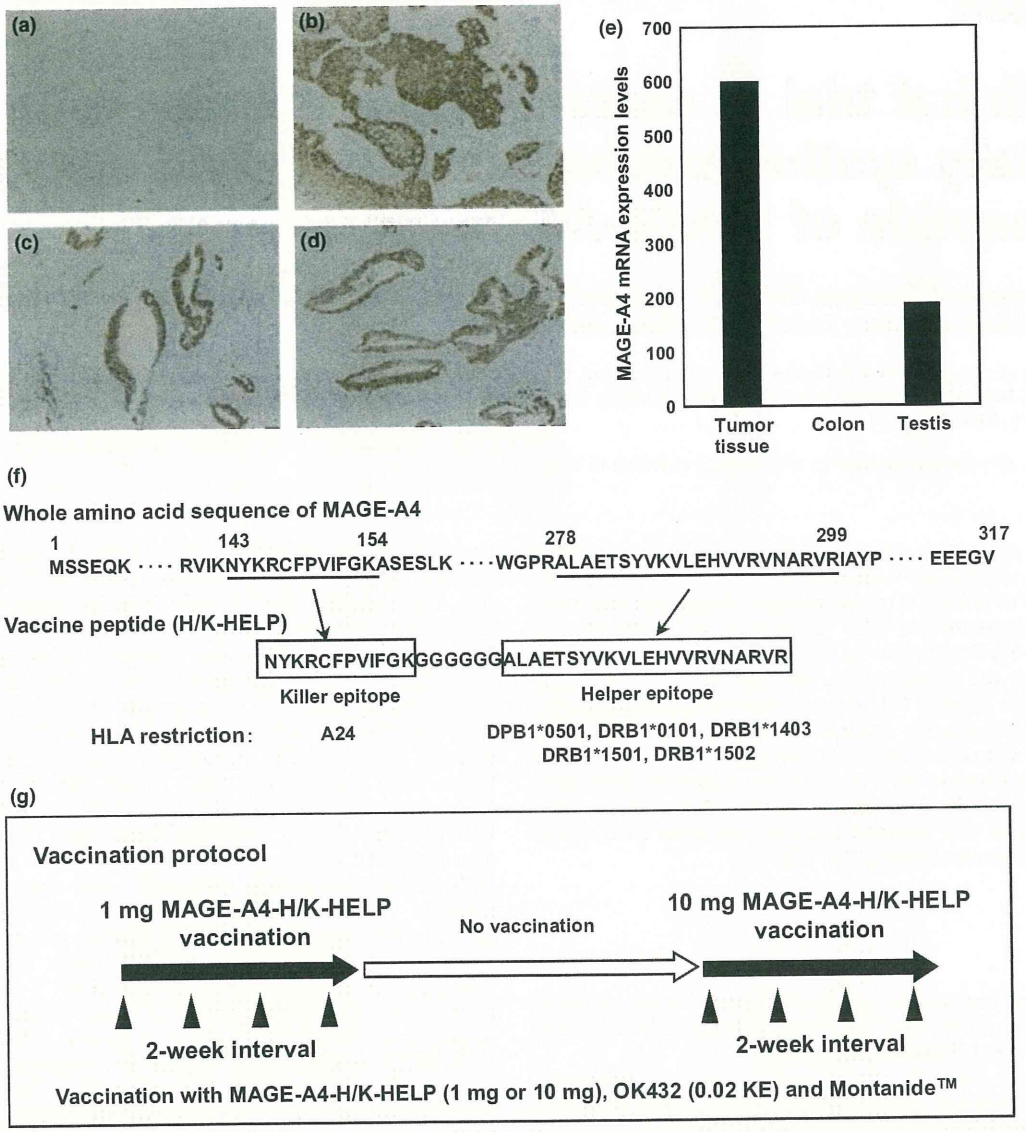

Fig. 1. Treatment of a patient with pulmonary metastasis of colon cancer with MAGE-A4-H/K-HELP. Immunohistochemical staining with anti-pan MAGE-A4 mAb (57B) for (a) MAGE-A4$^-$ bladder cancer (negative control), (b) head and neck cancer (positive control), which revealed similar staining intensity to testis, and (c, d) a tumor tissue sample of the enrolled patient. (e) MAGE-A4 mRNA expression levels were assessed by real-time PCR. Normal colon and testis were used as a negative or positive control, respectively. (f) The amino acid sequence of artificially synthesized MAGE-A4-H/K-HELP used in this trial. MAGE-A4-H/K-HELP was artificially synthesized by conjugating MAGE-A4$_{278-299}$ helper epitope (22 amino acid sequence in the right box) with MAGE-A4$_{143-154}$ killer epitope (12 amino acid sequence in the left box) by a glycine linker. (g) Vaccination protocol for the patient in a phase I study. The patient was vaccinated with 1 or 10 mg MAGE-A4-H/K-HELP mixed with OK-432 (0.02KE) and Montanide ISA-51 four times at 2-week intervals. H/K-HELP, helper/killer-hybrid epitope long peptide; HLA, human leukocyte antigen.

stimulated CD4$^+$ T cells and a part of the helper epitope peptide also activated CD8$^+$ T cells, while the MAGE-A4$_{143-154}$ killer epitope triggered the production of MAGE-A4-specific IgG Ab, indicating the long peptide vaccine, H/K-HELP, appeared to be beneficial for inducing both cellular and humoral immune responses in the cancer patient. In parallel with superior immune responses, tumor growth and serum levels of the carcinoembryonic antigen tumor marker were slightly decreased during cancer vaccine therapy with MAGE-A4-H/K-HELP (Fig. 3), and this patient's clinical response was finally judged as stable disease (Response Evaluation Criteria in Solid Tumors [RECIST] v1.1 guidelines[1]). This is the first report that cancer vaccine therapy with artificially synthesized MAGE-A4-H/K-HELP induced Th1-dependent cellular and humoral immune responses in a cancer patient. So far, no severe side-effects were observed in six patients treated with MAGE-A4-H/K-HELP (three patients with 1 mg and three patients with 10 mg, CTCAEv4.0), and significant T-cell responses were demonstrated in 50% of patients (data not shown).

Discussion

Cancer vaccine therapy using HLA class I-binding 8–9 amino acids short cancer peptide has been performed to induce cancer-specific cytotoxic T lymphocytes (CTL) in cancer patients.[2,3] Although cancer vaccine therapy with short peptide induced increased tetramer$^+$ cancer-specific CTL and long stable disease, the vaccine therapy focused only on CTL activation appears to be suboptimal in conquering cancer.[4–6] This might be because

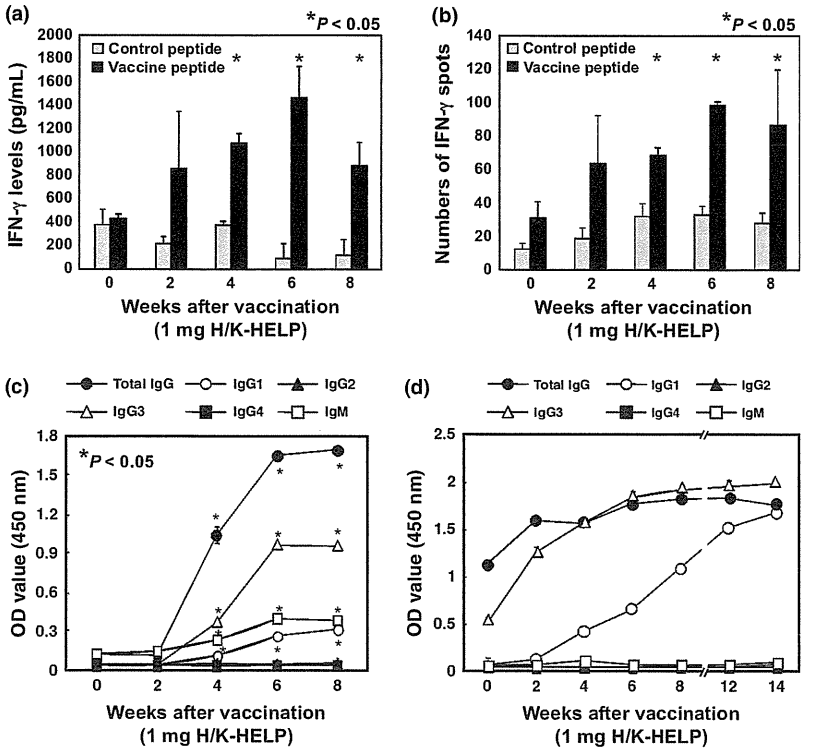

Fig. 2. Cellular and humoral immune responses in a patient vaccinated with MAGE-A4-H/K-HELP. (a,b) MAGE-A4-H/K-HELP-specific interferon (IFN)-γ production by $CD4^+$ T cells or $CD8^+$ T cells was assessed at various weeks after vaccination with MAGE-A4-H/K-HELP (1 mg) by ELISA (a) or enzyme-linked immunosorbent spot (ELISPOT) assay (b), respectively. *$P < 0.05$, against control survivin-H/K-HELP peptide. (c) The levels of antibodies (total IgG, ●; IgG1, ○; IgG2, ▲; IgG3, △; IgG4, ■; and IgM, □) against MAGE-A4-H/K-HELP peptide in the patient's serum sample (400-fold diluted) was determined at 2, 4, 6 and 8 weeks after vaccination with 1 mg MAGE-A4-H/K-HELP. *$P < 0.05$, against 0 weeks after vaccination. (d) The levels of antibodies (total IgG, ●; IgG1, ○; IgG2, ▲; IgG3, △; IgG4, ■; and IgM, □) against MAGE-A4-H/K-HELP peptide in the patient's serum sample (400-fold diluted) was determined at 2, 4, 6, 8, 10 and 12 weeks after vaccination with 10 mg MAGE-A4-H/K-HELP. H/K-HELP, helper/killer-hybrid epitope long peptide.

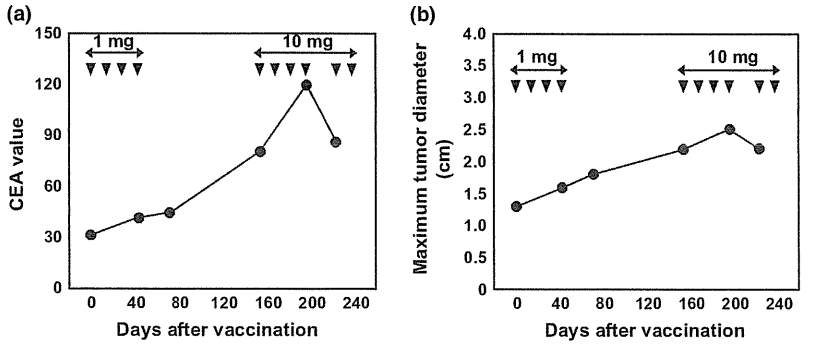

Fig. 3. Clinical responses in a colon cancer patient treated with MAGE-A4-H/K-HELP vaccine. (a) The carcinoembryonic antigen (CEA) value in the patient's serum was measured using ELISA on various days after vaccination. (b) Maximum tumor diameter was measured by computer tomography. H/K-HELP, helper/killer-hybrid epitope long peptide.

of the existence of strong immunosuppressive tumor escape mechanisms and the lack of helper T-cell activation.[7,8]

Therefore, it is essential to develop an efficient method to overcome immunosuppression to combat cancer. We initially demonstrated the critical role of Th1 and Th2 immunity in the tumor-bearing host and have proposed that the introduction of Th1-dominant immunity is essential for inducing fully activated CTL and immunological memory.[8–11] Recently, it has been demonstrated that a mixture of various synthetic long peptides (SLP) derived from the naturally occurring sequence of human papilloma virus (HPV)-16 oncoproteins was superior to short tumor peptides in terms of inducing a complete or partial response in vulvar intraepitheral neoplasia.[12] Zwaveling *et al.*[13] also reported that HPV-16-derived 35 amino acid-long peptide eradicated the established HPV-16-expressing mouse tumor. Thus, long peptide vaccine containing both helper and killer epitopes appeared to be a rational strategy to activate Th1-dependent antitumor immunity.[8] In contrast to viral-related

doi: 10.1111/j.1349-7006.2011.02106.x

cancer antigenic long peptide, p53-long peptide vaccine induced no complete or partial response in a clinical trial of human cancers, although it induced significant T cell responses.[14,15] Moreover, the first clinical trial using a synthetic 15 amino acid peptide vaccine containing a naturally occurring combination of helper and killer epitopes of $gp100_{175-189}$ exhibited no significant impact for therapeutic efficacy of melanoma.[16] Therefore, what kinds of long peptide induce a beneficial therapeutic effect against human cancer still remains unclear.

Here, we prepared an artificially synthesized long peptide, which conjugate MAGE-A4 class I-binding epitope and our defined helper epitope,[17] and applied it to a patient with pulmonary metastatic colon cancer. In contrast to short $gp100_{175-189}$ peptide including helper and killer epitopes,[16] we successfully induced cancer-specific Th1/Tc1 cells and complement-fixing Ab (IgG1 and IgG3)[18] by 40 amino acid H/K-HELP. This discrepancy might be because artificially synthesized 40 amino acid-long peptide but not short peptide has a beneficial structure for inducing favorable dendritic cells (DC) presentation and subsequent activation of Th1 and Tc1 cells.

Bijker *et al.*[19] reported that SLP of class I-binding long cancer peptide was efficiently processed by professional APC and subsequently exhibited a sustained stimulating activity of DC to induce Th-dependent, tumor-specific CTL.[19] We have also confirmed that ovalbumin (OVA)-H/K-HELP was superior to short peptide in curing mice with OVA-expressing tumor (data not shown). In another clinical trial, we demonstrated that survivin-H/K-HELP induced a complete response in a breast cancer patient (data not shown). Thus, we believe that artificially synthesized H/K-HELP of cancer antigen will become a promising tool to induce Th1-dependent cellular and humoral immunity in cancer patients, as well as SLP derived from natural tumor-associated HPV-16 antigen peptide.[12]

Acknowledgments

The authors thank the patient for consenting to the publication of their clinical details. The authors are also grateful to the clinical research coordinators of Hokkaido University Hospital for their support with the treatment of the patient. This study is part of a ''Development of Innovative Cancer Immunotherapy by Helper T cells'', sponsored by a Translational Research Promotion Project of the New Energy and Industrial Technology Development Organization (NEDO).

Disclosure Statement

All authors declare that they have no conflict of interest.

References

1 Eisenhauer EA, Therasse P, Bogaerts J *et al.* New response evaluation criteria in solid tumors: revised RECIST guideline (version 1.1). *Eur J Cancer* 2009; **45**: 228–47.
2 van der Bruggen P, Traversari C, Chomez P *et al.* A gene encoding an antigen recognized by cytolytic T lymphocytes on a human melanoma. *Science* 1991; **254**: 1643–7.
3 Simpson AJ, Caballero OL, Jungbluth A, Chen YT, Old LJ. Cancer/testis antigens, gametogenesis and cancer. *Nat Rev Cancer* 2005; **5**: 615–25.
4 Rosenberg SA, Yang JC, Restifo NP. Cancer immunotherapy: moving beyond current vaccines. *Nat Med* 2004; **10**: 909–15.
5 Hattori T, Mine T, Komatsu N *et al.* Immunological evaluation of personalized peptide vaccination in combination with UFT and UZEL for metastatic colorectal carcinoma patients. *Cancer Immunol Immunother* 2009; **58**: 1843–52.
6 Noguchi M, Mine T, Komatsu N *et al.* Assessment of immunological biomarkers in patients with advanced cancer treated by personalized peptide vaccination. *Cancer Biol Ther* 2011; **10**: 1266–79.
7 Nishikawa H, Kato T, Tawara I *et al.* Accelerated chemically induced tumor development mediated by CD4+CD25+ regulatory T cells in wild-type hosts. *Proc Natl Acad Sci USA* 2005; **102**: 9253–7.
8 Nishimura T, Iwakabe K, Sekimoto M *et al.* Distinct role of antigen-specific T helper type 1 (Th1) and Th2 cells in tumor eradication in vivo. *J Exp Med* 1999; **190**: 617–27.
9 Takeshima T, Chamoto K, Wakita D *et al.* Local Radiation Therapy Inhibits Tumor Growth through the Generation of Tumor-Specific CTL: its Potentiation by Combination with Th1 Cell Therapy. *Cancer Res* 2010; **70**: 2697–706.
10 Hunder NN, Wallen H, Cao J *et al.* Treatment of metastatic melanoma with autologous CD4+ T cells against NY-ESO-1. *N Engl J Med* 2008; **358**: 2698–703.
11 Kobayashi H, Celis E. Peptide epitope identification for tumor-reactive CD4 T cells. *Curr Opin Immunol* 2008; **20**: 221–7.
12 Kenter GG, Welters MJ, Valentijn AR *et al.* Vaccination against HPV-16 oncoproteins for vulvar intraepithelial neoplasia. *N Engl J Med* 2009; **361**: 1838–47.
13 Zwaveling S, Ferreira Mota SC, Nouta J *et al.* Established human papillomavirus type 16-expressing tumors are effectively eradicated following vaccination with long peptides. *J Immunol* 2002; **169**: 350–8.
14 Speetjens FM, Kuppen PJ, Welters MJ *et al.* Induction of p53-specific immunity by a p53 synthetic long peptide vaccine in patients treated for metastatic colorectal cancer. *Clin Cancer Res* 2009; **15**: 1086–95.
15 Leffers N, Vermeij R, Hoogeboom BN *et al.* Long-term clinical and immunological effects of p53-SLP® vaccine in patients with ovarian cancer. *Int J Cancer* 2011; doi: 10.1002/ijc.25980 [Epub ahead of print].
16 Celis E, Center MSGotMCC. Overlapping human leukocyte antigen class I/II binding peptide vaccine for the treatment of patients with stage IV melanoma: evidence of systemic immune dysfunction. *Cancer* 2007; **110**: 203–14.
17 Ohkuri T, Wakita D, Chamoto K, Togashi Y, Kitamura H, Nishimura T. Identification of novel helper epitopes of MAGE-A4 tumour antigen: useful tool for the propagation of Th1 cells. *Br J Cancer* 2009; **100**: 1135–43.
18 Michaelsen TE, Garred P, Aase A. Human IgG subclass pattern of inducing complement-mediated cytolysis depends on antigen concentration and to a lesser extent on epitope patchiness, antibody affinity and complement concentration. *Eur J Immunol* 1991; **21**: 11–6.
19 Bijker MS, van den Eeden SJ, Franken KL, Melief CJ, van der Burg SH, Offringa R. Superior induction of anti-tumor CTL immunity by extended peptide vaccines involves prolonged, DC-focused antigen presentation. *Eur J Immunol* 2008; **38**: 1033–42.

Carcinogenesis vol.32 no.7 pp.995–1004, 2011
doi:10.1093/carcin/bgr068
Advance Access publication April 7, 2011

TRIM40 promotes neddylation of IKKγ and is downregulated in gastrointestinal cancers

Keita Noguchi[1,2], Fumihiko Okumura[1], Norihiko Takahashi[2], Akihiko Kataoka[2], Toshiya Kamiyama[2], Satoru Todo[2] and Shigetsugu Hatakeyama[1,*]

[1]Department of Biochemistry and [2]Department of General Surgery, Hokkaido University Graduate School of Medicine, N15, W7, Kita-ku, Sapporo, Hokkaido 060-8638, Japan

*To whom correspondence should be addressed. Tel: +81 11 706 5899; Fax: +81 11 706 5169;
Email: hatas@med.hokudai.ac.jp

Gastrointestinal neoplasia seems to be a common consequence of chronic inflammation in the gastrointestinal epithelium. Nuclear factor-kappaB (NF-κB) is an important transcription factor for carcinogenesis in chronic inflammatory diseases and plays a key role in promoting inflammation-associated carcinoma in the gastrointestinal tract. Activation of NF-κB is regulated by several posttranslational modifications including phosphorylation, ubiquitination and neddylation. In this study, we showed that tripartite motif (TRIM) 40 is highly expressed in the gastrointestinal tract and that TRIM40 physically binds to Nedd8, which is conjugated to target proteins by neddylation. We also found that TRIM40 promotes the neddylation of inhibitor of nuclear factor kappaB kinase subunit gamma, which is a crucial regulator for NF-κB activation, and consequently causes inhibition of NF-κB activity, whereas a dominant-negative mutant of TRIM40 lacking the RING domain does not inhibit NF-κB activity. Knockdown of TRIM40 in the small intestinal epithelial cell line IEC-6 caused NF-κB activation followed by increased cell growth. In addition, we found that TRIM40 is highly expressed in normal gastrointestinal epithelia but that TRIM40 is downregulated in gastrointestinal carcinomas and chronic inflammatory lesions of the gastrointestinal tract. These findings suggest that TRIM40 inhibits NF-κB activity via neddylation of inhibitor of nuclear factor kappaB kinase subunit gamma and that TRIM40 prevents inflammation-associated carcinogenesis in the gastrointestinal tract.

Introduction

Tripartite motif (TRIM) proteins are characterized by the presence of a RING finger, one or two zinc-binding motifs named B-boxes and an associated coiled-coil region (1). Most TRIM proteins have been reported to have a role in the ubiquitination process. TRIM25/estrogen-responsive finger protein ubiquitinates 14-3-3σ (2) and retinoic acid-inducible gene I (3). Furthermore, several TRIM family members are involved in various cellular processes, such as transcriptional regulation, cell growth, apoptosis, development and oncogenesis (4–8).

Neural precursor cell-expressed developmentary downregulated gene 8 (Nedd8) is a small ubiquitin-like protein with 53% identity to ubiquitin that is conserved from yeast to mammals (9–11). Nedd8 is covalently linked to the ε-amino group of lysine residues on target proteins through its C-terminal group as well as a ubiquitination reaction. Nedd8 is first activated by a heterodimeric E1 enzyme, APPBP1-Uba3 and is then transferred to an E2 enzyme, Ubc12. Members of the cullin family are well-characterized substrates for Nedd8 conjugation (10,12,13). Tumor suppressor protein p53 and its relative p73 are also neddylated via a RING domain containing protein Mdm2 or F-box domain protein FBXO11, and neddylation of p53 causes inhibition of p53-mediated transcription (14–16). Similarly, c-Cbl mediates epidermal growth factor receptor modification with Nedd8, which enhances subsequent ubiquitination, followed by degradation (17). A well-characterized component of a Cul2-based ubiquitin E3, von Hippel-Lindau protein, is also neddylated, and Nedd8 modification of von Hippel-Lindau protein regulates VHL-associated tumorigenesis (18). Several ribosomal proteins and breast cancer-associated protein3 (BCA3) are modified and regulated by Nedd8 (19,20). Taken together, although neddylation does not directly mediate proteasomal degradation of target proteins like ubiquitination, Nedd8 modification probably regulates several cellular functions including transcription, translation and signal transductions via structural change or stabilization of target proteins.

The nuclear factor-kappaB (NF-κB)-signaling pathway plays a key role in many aspects of cancer initiation and progression through transcriptional control of genes involved in growth, angiogenesis, anti-apoptosis, invasiveness and metastasis (21). Regulation of NF-κB signaling occurs at many levels, one of which is through the regulation of protein turnover by the action of SCF complex ubiquitin ligase. Under a resting condition, NF-κB is maintained in an inactive state by binding to IκB proteins. In canonical NF-κB signaling, IκBα binds to p50–p65 and sequesters transcription factors in the cytoplasm, rendering them inactive. On stimulation of the IKK complex, IκBα is phosphorylated at Serine 32 and Serine 36, resulting in its polyubiquitination by a ubiquitin ligase complex, SCF^{Fbw1} (Skp1-Cul1-F-box complex containing Fbw1), and degradation, thus resulting in nuclear accumulation of the complex and transcription of NF-κB target genes (22–25).

Chronic inflammation in the gastrointestinal tract has been closely associated with carcinogenesis (26). The most extensively studied examples are relationships between chronic gastritis resulting from *Helicobacter pylori* infection and gastric cancer, chronic hepatitis and liver cancer and chronic inflammatory bowel disease and colorectal cancer. Emerging evidence in the past decade has suggested that the NF-κB play a critical role in linking inflammation and cancer. NF-κB regulates major inflammatory factors including tumor necrosis factor (TNF) α, interleukin (IL)-6, IL-1, IL-8, many of which are also potent activators for NF-κB. It is thus probably that NF-κB and inflammation constitute a positive feedback loop in the milieu of inflammatory sites to induce cellular and DNA damage, promote cell proliferation and transformation, and eventually cause initiation, promotion and progression of cancer (27–30).

In this study, we showed that the TRIM family protein TRIM40 is highly expressed in the gastrointestinal tract including the stomach, small intestine and large intestine. With the aim of elucidating the molecular function of TRIM40 in the gastrointestinal tract, we identified Nedd8 as a novel TRIM40-binding protein by using yeast two hybrid screening. TRIM40 enhanced neddylation of IKKγ and inhibited the activity of NF-κB-mediated transcription. We also found that knockdown of TRIM40 causes NF-κB activation and increases cell growth. These results provide evidence for a protective role of TRIM40 in inflammation and carcinogenesis in the gastrointestinal tract.

Materials and methods

Cell culture

HEK293T, HeLa and SW480 cell lines were cultured under an atmosphere of 5% CO_2 at 37°C in Dulbecco's modified Eagle's medium (Sigma Chemical Co, St Louis, MO) supplemented with 10% fetal bovine serum (Invitrogen, Carlsbad, CA). IEC-6 cell line was cultured under the same conditions in Dulbecco's modified Eagle's medium supplemented with 10% fetal bovine serum and 0.1 U/ml bovine insulin (Sigma).

Abbreviations: cDNA, complementary DNA; IL, interleukin; mRNA, messenger RNA; Nedd8, neural precursor cell-expressed developmentary downregulated gene 8; NF-κB, nuclear factor-kappaB; PBS, phosphate-buffered saline; PCR, polymerase chain reaction; TRIM, tripartite motif.

Cloning of complementary DNAs and plasmid construction

Human *TRIM40* complementary DNAs (cDNAs) were amplified from human stomach cDNA by polymerase chain reaction (PCR) with KOD-Plus- (Toyobo, Osaka, Japan) using the following primers: 5′-atgatccctttgcagaaggac-3′ (Hs-TRIM40-sense) and 5′-tcagagcttctgaggggctg-3′ (Hs-TRIM40-antisense). Mouse *TRIM40* cDNA was amplified from mouse small intestine cDNA by PCR with KOD-Plus- (Toyobo) using the following primers: 5′-accatgggctctcttgacaaggac-3′ (Mm-TRIM40-sense) and 5′-agactaactgagctttggaccagc-3′ (Mm-TRIM40-antisense). The cDNA fragment lacking a sequence corresponding to amino acids 1–54 was utilized as TRIM40(ΔRING). The amplified fragments were subcloned into pBluescript II SK+ (Stratagene, La Jolla, CA). *TRIM40* cDNAs were subcloned into pCR-FLAG, pCGN-HA, pcDNA3-Myc (Invitrogen), pET30a (Merck, Frankfurt, Germany), pGEX-6P1 (GE Healthcare, Piscataway, NJ) and pBTM116 (Clontech, Mountain View, CA). Deletion mutants of mouse TRIM40 cDNA containing amino acids 55–247 were amplified by PCR and subcloned. Expression vectors encoding IKKα, IKKβ, IKKγ and Nedd8 cDNA were described previously (25).

Yeast two hybrid screening

cDNA encoding the full length of mouse *TRIM40* was fused in frame to the nucleotide sequence for the LexA domain (Clontech) in the yeast two hybrid vector pBTM116. To screen for proteins that interact with TRIM40, we transfected yeast strain L40 (Invitrogen) stably expressing the corresponding pBTM116 vector with a mouse NIH3T3 cDNA library (Clontech).

Antibodies and reagents

The antibodies used in this study were as follows: mouse monoclonal anti-HA (HA.11/16B12; Covance, Princeton, NJ), rabbit polyclonal anti-HA (Y11; Santa Cruz, Santa Cruz, CA), mouse monoclonal anti-FLAG (M2 or M5; Sigma), mouse monoclonal anti-c-Myc (9E10; Covance), mouse monoclonal anti-human IκBα (610690; BD Pharmingen, San Jose, CA), rabbit polyclonal anti-Nedd8 (PM023; BML, Tokyo, Japan), mouse monoclonal anti-IKKγ (K0159-3; BML), mouse monoclonal anti-Hsp70 (610608; BD), mouse monoclonal anti-p65 (610868; BD), mouse monoclonal anti-GAPDH (6C5; Ambion, Austin, TX), mouse monoclonal anti-lamin A/C (612162; BD) and mouse monoclonal anti-β-actin (AC15; Sigma). TNFα, IL-1β and cycloheximide were purchased from Sigma.

Transfection, immunoprecipitation and immunoblot analysis

HEK293T cells were transfected by the calcium phosphate method and lysed in a solution containing 50 mmol/l Tris–HCl (pH 7.4), 150 mmol/l NaCl, 1% Triton X-100, leupeptin (10 μg/ml), 1 mmol/l phenylmethylsulfonyl fluoride, 400 μmol/l Na_3VO_4, 400 μmol/l ethylenediaminetetraacetic acid, 10 mmol/l NaF and 10 mmol/l sodium pyrophosphate. The cell lysates were centrifuged at 15 000*g* for 10 min at 4°C, and the resulting supernatant was incubated with antibodies for 2 h at 4°C. Protein A-sepharose (GE Healthcare) that had equilibrated with the same solution was added to the mixture, which was then rotated for 1 h at 4°C. The resin was separated by centrifugation, washed five times with ice-cold lysis buffer and then boiled in sodium dodecyl sulfate sample buffer. Immunoblot analysis was performed with primary antibodies, horseradish peroxidase-conjugated antibodies to mouse or rabbit IgG (1:10 000 dilution; Promega, Madison, WI) and an enhanced chemiluminescence system (GE Healthcare). Subcellular fractionation was performed as reported previously (31).

Dual-luciferase assay

HEK293T, HeLa, SW480 and IEC-6 cells were seeded in 24-well plates at 1×10^5 cells per well and incubated at 37°C with 5% CO_2 for 24 h. NF-κB luciferase reporter plasmid and pRL-TK Renilla luciferase plasmid (Promega) were transfected into HEK293T, HeLa, SW480 and IEC-6 cells using the Fugene HD reagent (Roche, Basel, Switzerland). Twenty-four hours after transfection, cells were incubated with TNFα (20 ng/ml) for 6 h, harvested and assayed by the Dual-Luciferase Reporter Assay System (Promega). The luminescence was quantified with a luminometer (Tuner Designs, Sunnyvale, CA).

Immunofluorescence staining

HeLa cells expressing HA-tagged TRIM40 on a glass cover were fixed by phosphate-buffered saline (PBS) containing 4% formaldehyde and 0.1% Triton X-100 for 10 min at room temperature, followed by incubation with PBS containing anti-HA antibody (Y-11, 1 μg/ml), anti-FLAG antibody (M5, 1 μg/ml) and anti-p65 antibody (BD, 1 μg/ml) with 0.1% bovine serum albumin and 0.1% saponin for 1 h at room temperature. Cells were washed three times with PBS, followed by incubation with PBS containing Alexa546-labeled goat anti-mouse IgG antibody, Alexa488-labeled goat anti-rabbit IgG antibody, Alexa546-labeled goat anti-rabbit IgG antibody or Alexa488-labeled goat anti-mouse IgG antibody (Invitrogen) with 0.1% bovine serum albumin and 0.1% saponin for 1 h at room temperature. The cells were further incubated with Hoechst 33258 (1 μg/ml) in PBS for 10 min, followed by extensive washing with PBS and then photographed with a CCD camera (DP71; Olympus, Tokyo, Japan) attached to an Olympus BX51 microscope.

Recombinant proteins

Glutathione S-transferase-tagged TRIM40 was expressed in XL-10 cells and then purified by reduced glutathione–sepharose beads (Roche). His_6/FLAG-tagged TRIM40 was expressed in *Escherichia coli* strain BL21 (DE3; Invitrogen) and then purified by using ProBond metal affinity beads (Invitrogen).

Retroviral expression system

Wild-type FLAG-TRIM40 or FLAG-TRIM40(ΔRING) cDNA was subcloned into pMX-puro. Retroviral expression vectors were kindly provided by Dr Kitamura (University of Tokyo). For retrovirus-mediated gene expression, HeLa cells were infected with retroviruses produced by Plat-A packaging cells. Cells were then cultured in the presence of puromycin (5 μg/ml).

RNA interference

pSUPER-retro-puro containing a non-functional random sequence (5′-cagtcgcgtttgcgactgg-3′) or the nucleotides 570–588 of rat *TRIM40* cDNA (5′-cttctctgaggcagtaaca-3′) was constructed according to the protocol of the manufacturer (OligoEngine, Seattle, WA). For retrovirus-mediated gene expression, IEC-6 cells were infected with retroviruses produced by Plat-E packaging cells. Cells were then cultured in the presence of puromycin (2 μg/ml).

Quantitative PCR analysis

Total RNA was isolated from human samples with the use of an ISOGEN (Nippon Gene, Tokyo, Japan), followed by reverse transcription by ReverTra Ace (Toyobo). The resulting cDNA was subjected to real-time PCR with a StepOne machine and Power SYBR Green PCR master mix (Applied Biosystems, Foster City, CA). The level of gene expression relative to *GAPDH* was determined. The primer sequences for human *GAPDH* (GenBankTM accession number NM_002046.3) and human *TRIM40* (GenBankTM accession number NM_138700.3) were as follows: human *GAPDH*, 5′-gcaaattccatggcaccgt-3′ and 5′-tcgccccacttgattttgg-3′ and human *TRIM40*, 5′-caacacactgaagaatgctgg-3′ and 5′-cttctgaggggctgaagaag-3′. The primer sequences for rat *GAPDH* (GenBankTM accession number NM_017008.3) and rat *TRIM40* (GenBankTM accession number NM_001009175.1) were as follows: rat *GAPDH*, 5′-cacggcaagttcaacggcacagtca-3′ and 5′-gtgaagacgccagtagactccacgac-3′ and rat *TRIM40*, 5′-caccgggcccatactgagctc-3′ and 5′-ttcctgagccttcagccgttg-3′.

Human tissue samples

Tissues from patients who gave informed consent under the guidelines of the Hokkaido University Hospital Ethics Committee were used for this study. Excised samples from lesions and adjacent normal tissues were obtained within 3 h after the operation. All excised tissues were immediately placed in liquid nitrogen and stored at −80°C until further analysis.

Statistical analysis

The unpaired Student's *t*-test and Wilcoxon matched pairs test were used to determine the statistical significance of experimental data.

Results

TRIM40 expression in normal mouse tissues and mammalian cell lines

We and others have shown that some of the TRIM family members are selectively expressed in specific tissues and cell lines (1,6,7). Although several TRIM family members are known to be involved in various cellular processes, the functions of almost all TRIM family proteins have not been elucidated. In this study, we found human and mouse TRIM40 as a new member of the TRIM family and we analyzed the biological function of TRIM40. To examine the expression levels of TRIM40 in several normal tissues at the protein level, we generated a rabbit polyclonal anti-TRIM40 antibody using recombinant mouse TRIM40 protein and performed immunoblot analysis using several mouse normal tissues. Immunoblot analysis showed that TRIM40 is highly expressed in the gastrointestinal tract, heart and cerebellum and faintly in the testis (Figure 1A). To further analyze the expression of TRIM40 in detail, we prepared several gastrointestinal tissues including the esophagus, stomach, small intestine and large intestine. Immunoblot analysis using cell extracts from these tissues showed that TRIM40 is expressed highly in the small intestine, moderately in the stomach and faintly in the esophagus and large intestine

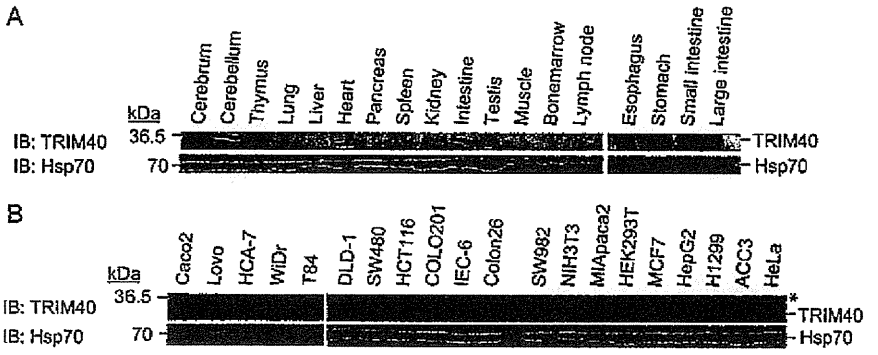

Fig. 1. Expression levels of TRIM40 in several mouse tissues and cell lines. (A) TRIM40 expression in several mouse tissues. The lysates from indicated mouse tissues were subjected to immunoblot (IB) analysis with anti-TRIM40 antibody and anti-Hsp70 antibody as a loading control. (B) TRIM40 expression in several cell lines. IB analysis with anti-TRIM40 or anti-Hsp70 antibody was performed using cell lysates from human intestine epithelial carcinoma cell lines Caco2, Lovo, HCA-7, WiDr, T84, DLD-1, SW480, HCT116 and COLO201, rat intestine epithelial cell line IEC-6, mouse colon epithelial carcinoma cell line Colon26, human synovial sarcoma cell line SW982, mouse embryonic fibroblast cell line NIH3T3, human pancreatic adenocarcinoma cell line MIApaca 2, human embryonic kidney cell line HEK293T, human breast carcinoma cell line MCF7, human hepatocellular carcinoma cell line HepG2, human lung carcinoma cell line H1299, human adenoid cystic carcinoma cell line ACC3 and human cervical carcinoma cell line HeLa. Asterisk represents non-specific band.

(Figure 1A). Furthermore, immunoblot analysis using several cell lines showed that TRIM40 is highly expressed in the rat small intestinal epithelial cell line IEC-6, the mouse colon adenocarcinoma cell line Colon26 and the human adenoid cystic carcinoma cell line ACC3, which are developmentally derived from parotid glands or gastrointestinal tissues (Figure 1B). These findings suggest that TRIM40 is more highly expressed in normal intestinal cells than in intestinal carcinoma cells.

TRIM40 interacts with Nedd8

To examine the molecular function of TRIM40, we isolated TRIM40-interacting proteins from an NIH 3T3 cDNA library by using a yeast two hybrid system. We obtained 16 positive clones from 1.2×10^6 transformants. Eight of the positive clones had sequence identities with cDNA encoding mouse Nedd8 (NCBI Reference Sequence: NM_008683.3). To examine whether TRIM40 physically interacts with Nedd8 in mammalian cells, we performed an *in vivo*-binding assay using cells transfected with expression vectors. We expressed FLAG-tagged TRIM40 together with Myc-tagged Nedd8 in HEK293T cells. Cell lysates were subjected to immunoprecipitation with an antibody to FLAG, and the resulting precipitates were subjected to immunoblot analysis with an antibody to Myc. Myc-tagged Nedd8 was coprecipitated by the antibody to FLAG, indicating that TRIM40 non-covalently interacts specifically with Nedd8 and also is covalently conjugated with Nedd8 (neddylation) (Figure 2A). We also confirmed interaction between FLAG-tagged TRIM40 lacking a RING domain [TRIM40(ΔRING)] and Myc-tagged Nedd8 by immunoprecipitation, suggesting that TRIM40(ΔRING) can be used as a null-functional mutant or a dominant-negative mutant (Figure 2A). Furthermore, immunoblot analysis using anti-Nedd8 antibody showed that overexpressed FLAG-tagged TRIM40 is covalently conjugated with Nedd8, but we could not show that overexpressed FLAG-tagged TRIM40 non-covalently interacts with Nedd8 (Figure 2A and B). These findings suggest that TRIM40 is covalently conjugated with Nedd8 and that TRIM40 weakly interacts with monomeric Nedd8.

TRIM40 inhibits NF-κB activity

It has been reported that Nedd8 covalently binds to and activates Cul1, which is a component of an SCF complex and that the SCF complex degrades IκBα phosphorylated by stimulation of TNFα, followed the activation of NF-κB-mediated transcription (12,13). To examine whether TRIM40 affects NF-κB activity, we performed an NF-κB response element luciferase reporter assay. We transfected expression vectors encoding TRIM40 with reporter plasmids into HEK293T cells. Six hours after stimulation with TNFα, luciferase activity was measured. The luciferase assays showed that TRIM40 suppressed NF-κB-mediated transcriptional activity in a dose-dependent fashion (Figure 2C). Furthermore, stable HeLa cell lines expressing FLAG-tagged TRIM40(WT) and FLAG-TRIM40(ΔRING) were generated by a retroviral expression system and luciferase assays were performed using these cell lines. Luciferase assays showed that overexpression of TRIM40 inhibits NF-κB activity compared with that of Mock, whereas overexpression of TRIM40(ΔRING) does not affect NF-κB activity, suggesting that a RING domain of TRIM40 is indispensable for inhibition of NF-κB activity (Figure 2D and E). In addition, we showed that TRIM40 also suppressed TNFα-induced NF-κB activity using the human colorectal adenocarcinoma cell line SW480 (Figure 2F). Since a canonical NF-κB pathway can be activated by many stimulations including stimulations with TNFα, IL-1β and lipopolysaccharide, a luciferase reporter assay using IL-1β was performed. The luciferase reporter assay showed that TRIM40 suppressed IL-1β-induced NF-κB activity (Figure 2G). These findings suggest that TRIM40 downregulates NF-κB-mediated transcriptional activity.

TRIM40 inhibits nuclear translocation of NF-κB

It has been reported that the p65 subunit of NF-κB is translocated from the cytoplasm to the nucleus upon stimulation with TNFα (32). To examine whether TRIM40 affects nuclear translocation of p65, immunofluorescent analysis was performed using an anti-p65 antibody. An expression vector encoding HA-tagged TRIM40 was transfected into HeLa cells, and the cells were stimulated with TNFα for 20 or 30 min and then stained with anti-p65 antibody. It was found that p65 was concentrated in the nucleus of mock cells by treatment with TNFα, whereas p65 was weakly concentrated in the nucleus of cells in which TRIM40 was highly expressed (Figure 3A and B). Immunofluorescent staining showed that overexpression of TRIM40 inhibits nuclear localization of endogenous p65 in HeLa cells by stimulation with TNFα, suggesting that TRIM40 inhibits a canonical NF-κB pathway (Figure 3A and B). The effect of TRIM40 on nuclear localization of endogenous p65 by TNFα was further confirmed by biochemical subcellular fractionation of HeLa cells. Immunoblotting with anti-p65 antibody was performed using each subcellular fraction from cells stimulated with TNFα. Endogenous p65 was mainly localized in the nucleus in mock cells by stimulation with TNFα, whereas half of the endogenous p65 remained in the cytosol in TRIM40-expressing cells, suggesting that TRIM40 inhibits nuclear translocation of p65 induced by stimulation with TNFα (Figure 3C and D).

TRIM40 stabilizes IκBα and interacts with IKK complex

Since we found that TRIM40 inhibits nuclear translocation of NF-κB and NF-κB-mediated transcriptional activity, we hypothesized that overexpression of TRIM40 would inhibit degradation of IκBα. To

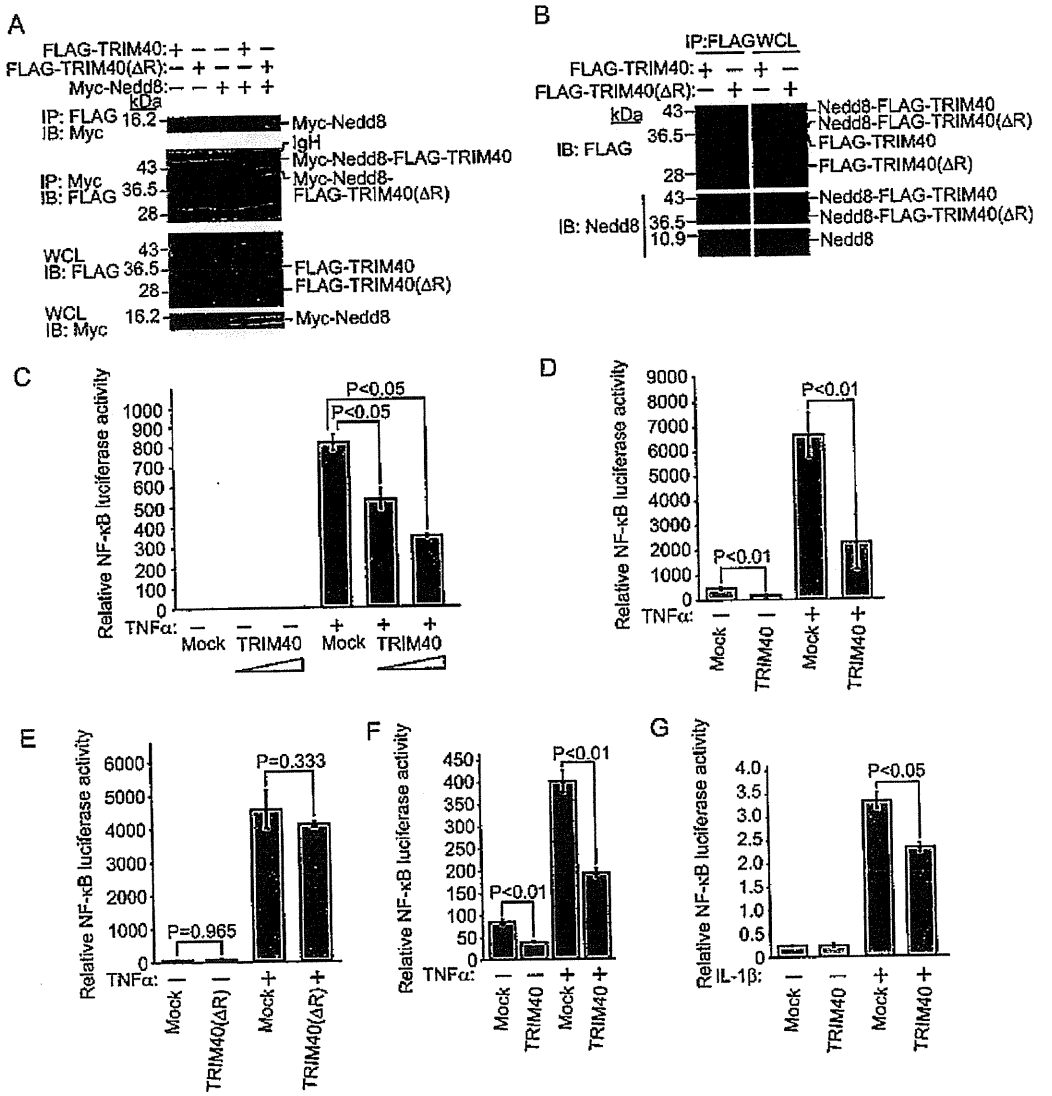

Fig. 2. TRIM40 interacts with Nedd8 and downregulates NF-κB activity. (**A**) *In vivo*-binding assay between TRIM40 and Nedd8. Expression vectors encoding FLAG-tagged TRIM40, FLAG-tagged TRIM40(ΔR) and Myc-tagged Nedd8 were transfected into HEK293T cells. Cell lysates (WCL) were immunoprecipitated with anti-FLAG or anti-Myc antibody and immunoblotted with anti-Myc and anti-FLAG antibodies. (**B**) *In vivo*-binding assay between TRIM40 and Nedd8. Expression vectors encoding FLAG-tagged TRIM40 and FLAG-tagged TRIM40 (ΔR) were transfected into HEK293T cells. Cell lysates (WCL) were immunoprecipitated with anti-FLAG antibody and immunoblotted with anti-FLAG and anti-Nedd8 antibodies. (**C**) TRIM40 reduces TNFα-induced NF-κB activity in a dose-dependent manner. HEK293T cells were transfected with the NF-κB luciferase reporter plasmid and an expression plasmid encoding TRIM40 (100 or 300 ng). Twenty-four hours after transfection, cells were treated with TNFα (20 ng/μl) and cultured for an additional 6 h. Data are means ± standard deviation of values from three independent experiments. The *P* values for the indicated comparisons were determined by Student's *t*-test. (**D**) Luciferase assay for NF-κB activity using HeLa cell lines stably expressing FLAG-tagged TRIM40. Stable cell lines were transfected with the NF-κB luciferase reporter plasmid. Twenty-four hours after transfection, cells were treated with TNFα (20 ng/μl) and cultured for an additional 6 h. (**E**) Luciferase assay for NF-κB activity using HeLa cell lines stably expressing FLAG-tagged TRIM40(ΔRING). Stable cell lines were transfected with the NF-κB luciferase reporter plasmid. Twenty-four hours after transfection, cells were treated with TNFα (20 ng/μl) and cultured for an additional 6 h and then luciferase activity was measured. R, RING domain. (**F**) TRIM40 reduces TNFα-induced NF-κB activity in the human colorectal adenocarcinoma cell line SW480. SW480 cells were transfected with the NF-κB luciferase reporter plasmid and an expression plasmid encoding TRIM40 (300 ng). Twenty-four hours after transfection, cells were treated with TNFα (20 ng/μl) and cultured for an additional 6 h and then luciferase activity was measured. (**G**) TRIM40 reduces IL-1β-induced NF-κB activity. HEK293T cells were transfected with the NF-κB luciferase reporter plasmid and an expression plasmid encoding TRIM40 (300 ng). Twenty-four hours after transfection, cells were treated with IL-1β (10 ng/μl) and cultured for an additional 6 h and then luciferase activity was measured.

examine whether overexpression of TRIM40 affects the stability of IκBα, an expression vector encoding TRIM40 was transfected. Immunoblot analysis clarified that overexpression of TRIM40 increases the stability of IκBα (Figure 4A). To further confirm that TRIM40 affects the stability of IκBα, a protein stability assay using cycloheximide was performed. HeLa cell lines stably expressing FLAG-tagged TRIM40 were stimulated with TNFα and incubated with cycloheximide for 0–60 min. The protein stability assay showed that stimulation with TNFα did not completely degrade IκBα even after 20 min of stimulation, suggesting that TRIM40 suppressed TNF-induced IκBα degradation (Figure 4B and C).

Next, we tested whether TRIM40 interacts with IKKα, IKKβ and IKKγ as upstream regulators for IκBα. We transfected expression vectors encoding HA-tagged TRIM40 or HA-tagged TRIM40(ΔRING) and FLAG-tagged IKKα, FLAG-tagged IKKβ or FLAG-tagged IKKγ into HEK293T cells. Cell lysates were

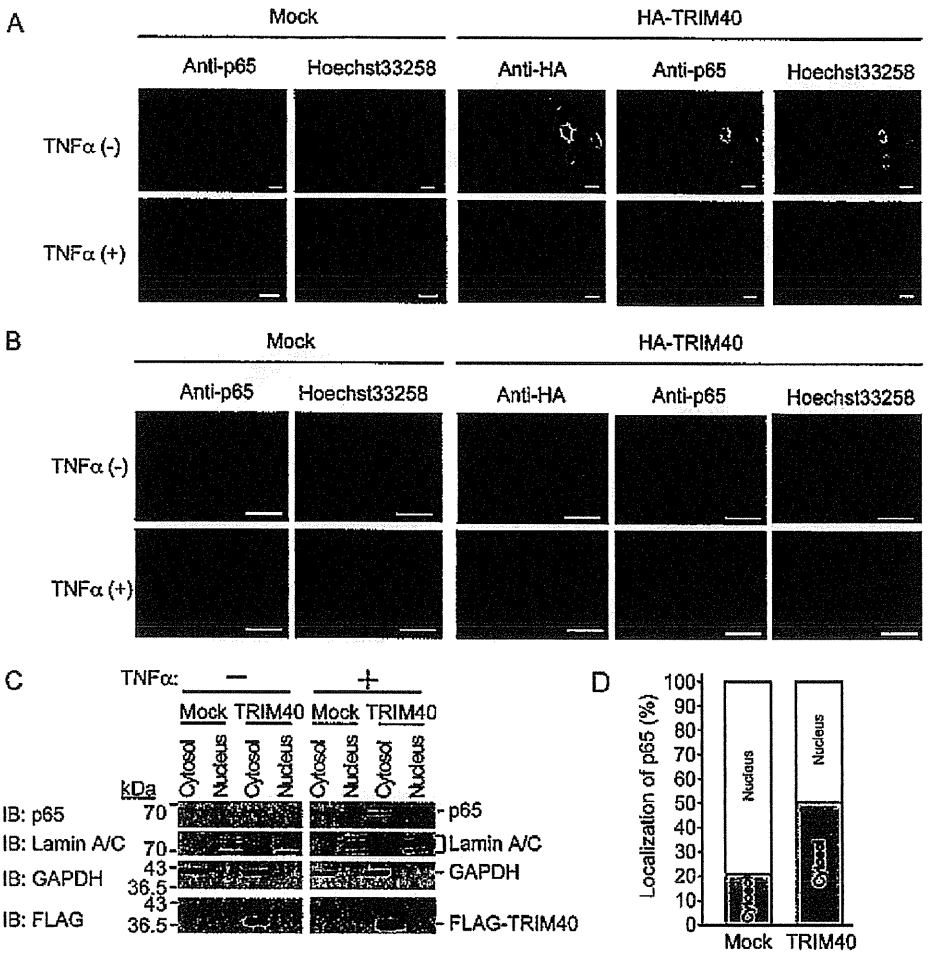

Fig. 3. TRIM40 inhibits translocation of p65 from the cytosol to the nucleus. (A) Immunofluorescent staining of p65 in TRIM40-overexpressing cells at low magification. HeLa cells were transfected with an expression plasmid encoding HA-tagged TRIM40. Forty-eight hours after transfection, the cells were stimulated with TNFα (20 ng/ml) for 20 min and were stained with anti-HA and anti-p65 antibodies, followed by incubation with Alexa488-labeled anti-rabbit IgG antibody and Alexa546-labeled anti-mouse IgG antibody, respectively. Nuclei were visualized using Hoechst 33258. Scale bars, 10 μm. **(B)** Immunofluorescent staining of p65 in TRIM40-overexpressing cells at high magnification. HeLa cells were transfected with an expression plasmid encoding HA-tagged TRIM40. Forty-eight hours after transfection, the cells were stimulated with TNFα (20 ng/ml) for 30 min and were stained with anti-HA and anti-p65 antibodies, followed by incubation with Alexa546-labeled anti-rabbit IgG antibody and Alexa488-labeled anti-mouse IgG antibody, respectively. Nuclei were visualized using Hoechst 33258. Scale bars, 10 μm. (C) Subcellular fractionation of p65 from TRIM40-overexpressing cells. HeLa cell lines stably expressing FLAG-tagged TRIM40 were stimulated with TNFα (20 ng/ml). Thirty minutes after stimulation, biochemically fractionated cytosolic and nuclear extracts were subjected to immunoblot analysis with anti-p65, anti-GAPDH and anti-Lamin A/C antibodies. GAPDH and lamin A/C are used as cytosolic and nuclear markers, respectively. (D) Quantification of p65 in cytosol or nuclear fractions. The intensities of p65 bands in (C) were quantified using a densitometer.

subjected to immunoprecipitation with an antibody to HA or FLAG, and the resulting precipitates were subjected to immunoblot analysis with an antibody to FLAG or HA, respectively. Immunoblot analysis showed that HA-tagged TRIM40 was selectively coprecipitated by anti-FLAG antibody and that FLAG-tagged IKKα, FLAG-tagged IKKβ and FLAG-tagged IKKγ were also coprecipitated by anti-HA antibody (Figure 4D, E and F). We also verified interaction between HA-tagged TRIM40(ΔRING) and FLAG-tagged IKKα, FLAG-tagged IKKβ or FLAG-tagged IKKγ by immunoprecipitation (Figure 4D, E and F). TRIM40(ΔR) interacts with IKK subunits much more strongly than TRIM40(WT) does (Figure 4D, E and F), suggesting that the RING domain may inhibit the interaction between TRIM40 and IKK subunits. These findings suggest that TRIM40 is contained in the IKK complex and inhibits the degradation of IκBα in a resting state.

TRIM40 is modified by Nedd8 and promotes neddylation of IKKγ

It has been reported that IKKγ is regulated by several posttranslational modifications including K63-linked or linear polyubiquitination (33,34). Since TRIM40 interacts with Nedd8 and IKKγ, we examined whether Nedd8 affects IKKγ by TRIM40. To examine whether TRIM40 exhibits Nedd8 conjugation on IKKγ, we performed an *in vivo* neddylation assay. Expression vectors encoding FLAG-tagged IKKγ, HA-tagged TRIM40, HA-tagged TRIM40(ΔRING) and Myc-tagged Nedd8 were transfected into HEK293T cells, and cell lysates were subjected to immunoprecipitation with an antibody to Myc and immunoblotted with an antibody to FLAG. Although FLAG-IKKγ was slightly neddylated even without overexpression of TRIM40, overexpression of TRIM40 considerably enhanced neddylation of FLAG-IKKγ (Figure 5A). Next, to elucidate in detail whether TRIM40 neddylates IKKγ, we performed an *in vivo* neddylation assay using several amounts of an expression vector HA-tagged TRIM40. Immunoblot analysis showed that TRIM40 enhances neddylation on IKKγ in a dose-dependent fashion (Figure 5B), suggesting that TRIM40 mediates neddylation on IKKγ and then possibly modulates kinase activity of the IKK complex, followed by stabilization of IκBα. Although immunoblot analysis of IKKα and IKKβ was

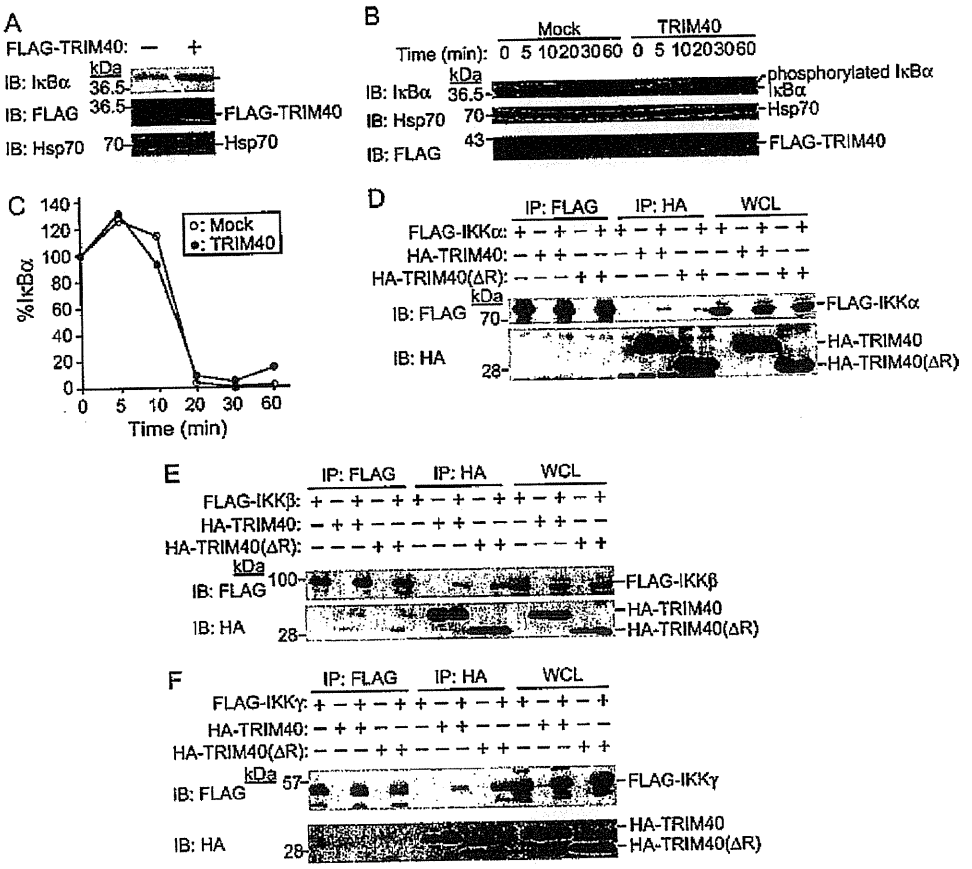

Fig. 4. TRIM40 interacts with IKK complex. (A) Upregulation of endogenous IκBα by TRIM40. Immunoblot analysis was performed using HeLa cells stably expressing FLAG-tagged TRIM40. Cell lysates were subjected to immunoblot (IB) analysis with anti-FLAG, anti-IκBα or anti-Hsp70 antibody. Anti-Hsp70 antibody was used as a loading control. (B) TRIM40 affects the stability of IκBα. HeLa cell lines stably expressing FLAG-tagged TRIM40 were stimulated with TNFα (20 ng/ml) and cycloheximide (25 μg/ml) for 0–60 min. Cell extracts were analyzed by immunoblotting with anti-IκBα antibody, anti-Hsp70 antibody and anti-FLAG antibody. Anti-Hsp70 antibody was used as a loading control. (C) Intensity of the IκBα bands in protein stability analysis in (B) was normalized by that of the corresponding Hsp70 bands and was then expressed as a percentage of the normalized value for time zero. (D) Interaction between IKKα and TRIM40. HEK293T cells were transfected with plasmids encoding FLAG-tagged IKKα, HA-tagged TRIM40 and HA-tagged TRIM40(ΔRING), followed by immunoprecipitation (IP) with anti-FLAG antibody or anti-HA antibody. Immunoprecipitates were subjected to IB analysis with anti-FLAG or anti-HA antibody. (E) Interaction between IKKβ and TRIM40. HEK293T cells were transfected with plasmids encoding FLAG-tagged IKKβ, HA-tagged TRIM40 and HA-tagged TRIM40(ΔRING), followed by IP with anti-FLAG antibody or anti-HA antibody. Immunoprecipitates were subjected to IB analysis with anti-FLAG or anti-HA antibody. (F) Interaction between IKKγ and TRIM40. HEK293T cells were transfected with plasmids encoding FLAG-tagged IKKγ, HA-tagged TRIM40 and HA-tagged TRIM40(ΔRING), followed by IP with anti-FLAG antibody or anti-HA antibody. Immunoprecipitates were subjected to IB analysis with anti-FLAG or anti-HA antibody.

performed, neddylation of IKKα and IKKβ was not observed (Figure 5C and D).

Knockdown of TRIM40 promotes activity of NF-κB and increases cell growth

To evaluate the physiological function of TRIM40, retroviral vectors encoding shRNA specific for rat *TRIM40* (shTRIM40) or non-targeting shRNA as a control (Mock) were infected into IEC-6 cells in which TRIM40 is highly expressed. After puromycin selection, a stable IEC-6 cell line in which TRIM40 is knocked down was established, and TRIM40 expression at protein and messenger RNA (mRNA) levels was confirmed by immunoblot analysis and quantitative real-time PCR, respectively (Figure 6A and B). Using these cell lines, we performed an NF-κB response element luciferase reporter assay. Six hours after stimulation with TNFα, luciferase activity was measured. The luciferase assays showed that knockdown of TRIM40 enhances NF-κB-mediated transcriptional activity (Figure 6C). Interestingly, knockdown of TRIM40 caused activation of NF-κB-mediated transcription even without TNFα stimulation. In addition, knockdown of TRIM40 increased cell growth (Figure 6D). These findings suggest that TRIM40 downregulates NF-κB-mediated transcriptional activity and that TRIM40 is an important regulator to prevent NF-κB activation in a resting state.

Since it has been reported that NF-κB activity is upregulated in gastrointestinal carcinomas, we investigated the expression of *TRIM40* mRNA in human cancers and inflammation (29,30). Quantitative real-time PCR was performed and mRNA expression levels of *TRIM40* were compared in gastrointestinal cancers (including Crohn's disease) and normal tissues. Expression levels of *TRIM40* mRNA were lower in samples of gastric cancer (13/13), colon cancer (3/3), rectal cancer (3/4), benign colon tumor (0/1) and Crohn's disease (1/1) than in normal epithelia. Quantitative real-time PCR showed that *TRIM40* mRNA is highly expressed in human normal gastrointestinal tissues and significantly downregulated in gastrointestinal carcinomas and inflammation (Figure 6E and F).

To verify Nedd8 conjugation of IKKγ in human gastrointestinal tissues, immunoprecipitation and immunoblot analysis were performed using normal gastric epithelium and gastric cancer tissue from the same patient. Cell lysates were subjected to immunoprecipitation with an antibody to anti-IKKγ or anti-Nedd8, and the resulting precipitates were subjected to immunoblot analysis with an antibody to anti-Nedd8 or anti-IKKγ, respectively. Neddylation of IKKγ was selectively detected in normal gastric epithelium (Figure 6F). These

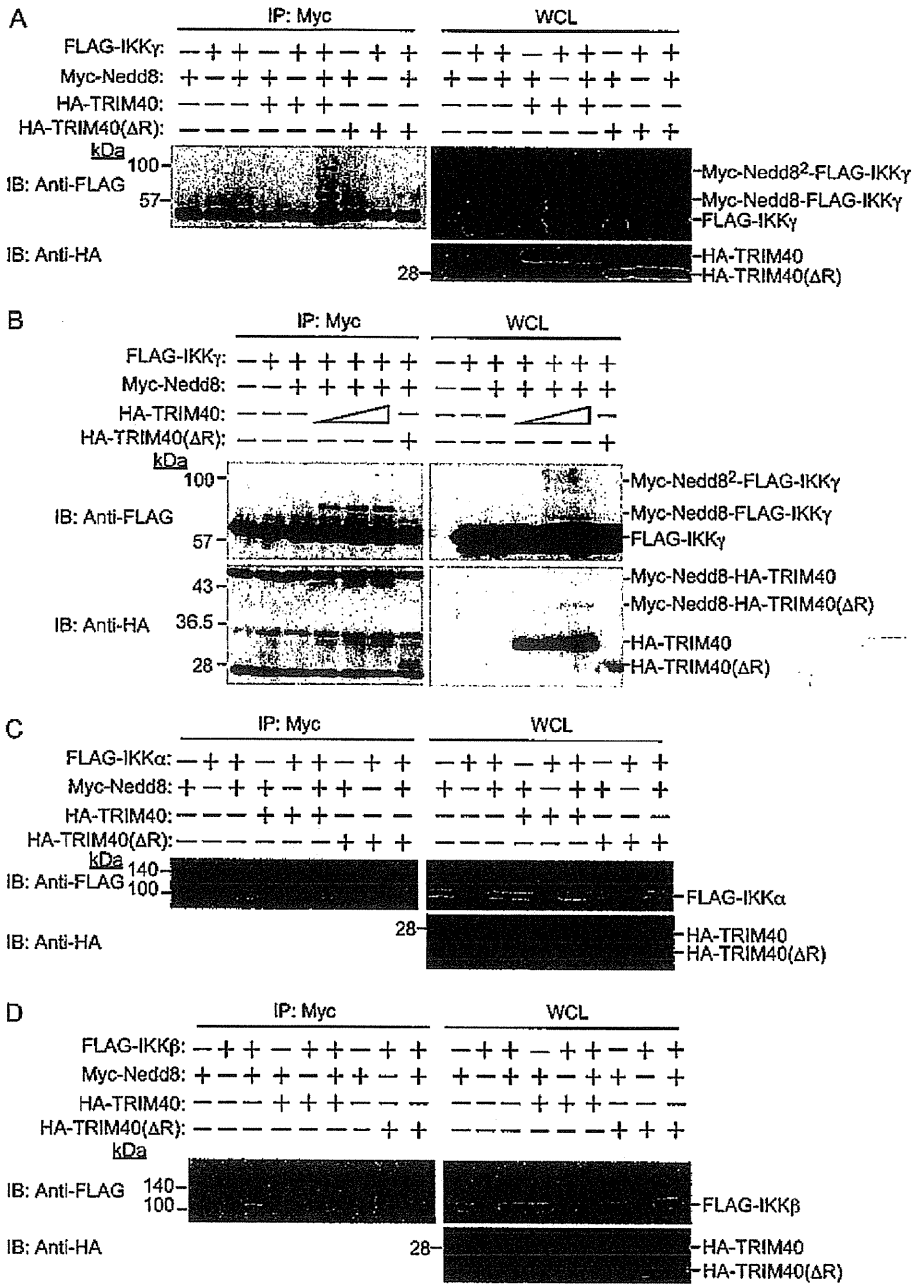

Fig. 5. TRIM40 promotes neddylation of IKKγ. (**A**) *In vivo* neddylation assay of IKKγ by TRIM40. HEK293T cells were transfected with plasmids encoding FLAG-tagged IKKγ, HA-tagged TRIM40, HA-tagged TRIM40 (ΔRING) and Myc-tagged Nedd8, followed by immunoprecipitation (IP) with anti-Myc antibody. Immunoprecipitates were subjected to immunoblot (IB) analysis with anti-FLAG or anti-HA antibody. (**B**) TRIM40 promotes neddylation of IKKγ in a dose-dependent fashion. HEK293T cells were transfected with plasmids encoding FLAG-IKKγ, HA-TRIM40 (1, 3 or 6 μg), HA-tagged TRIM40(ΔRING) (3 μg) and Myc-tagged Nedd8, followed by IP with anti-Myc antibody. Immunoprecipitates were subjected to IB analysis with anti-FLAG or anti-HA antibody. (**C** and **D**) *In vivo* neddylation assay of IKKα or IKKβ by TRIM40. HEK293T cells were transfected with plasmids encoding FLAG-tagged IKKα or IKKβ, HA-tagged TRIM40, HA-tagged TRIM40 (ΔRING) and Myc-tagged Nedd8, followed by IP with anti-Myc antibody. Immunoprecipitates were subjected to IB analysis with anti-FLAG or anti-HA antibody.

findings suggest that endogenous TRIM40 is highly expressed and promotes neddylation of IKKγ, resulting in stabilization of IκBα.

Discussion

In this study, we found that TRIM40 is highly expressed in gastrointestinal tissues and that TRIM40 interacts with the ubiquitin-like protein Nedd8. We focused on the relationship between TRIM40 and Nedd8 because Nedd8 conjugation regulates activity of NF-κB through the SCF complex (12). Although it has been reported that a subunit of SCF complex, Cul1, is positively regulated via Nedd8 conjugation, we did not find interaction of TRIM40 with the SCF complex (data not shown). We further investigated other steps for NF-κB activation and found that TRIM40 interacts with the IKK complex. We showed that overexpression of TRIM40 promotes neddylation of IKKγ and that TRIM40 causes stabilization of IκBα and attenuates NF-κB activity, whereas a mutant of TRIM40 lacking the RING-finger domain does not affect NF-κB activity. Furthermore,

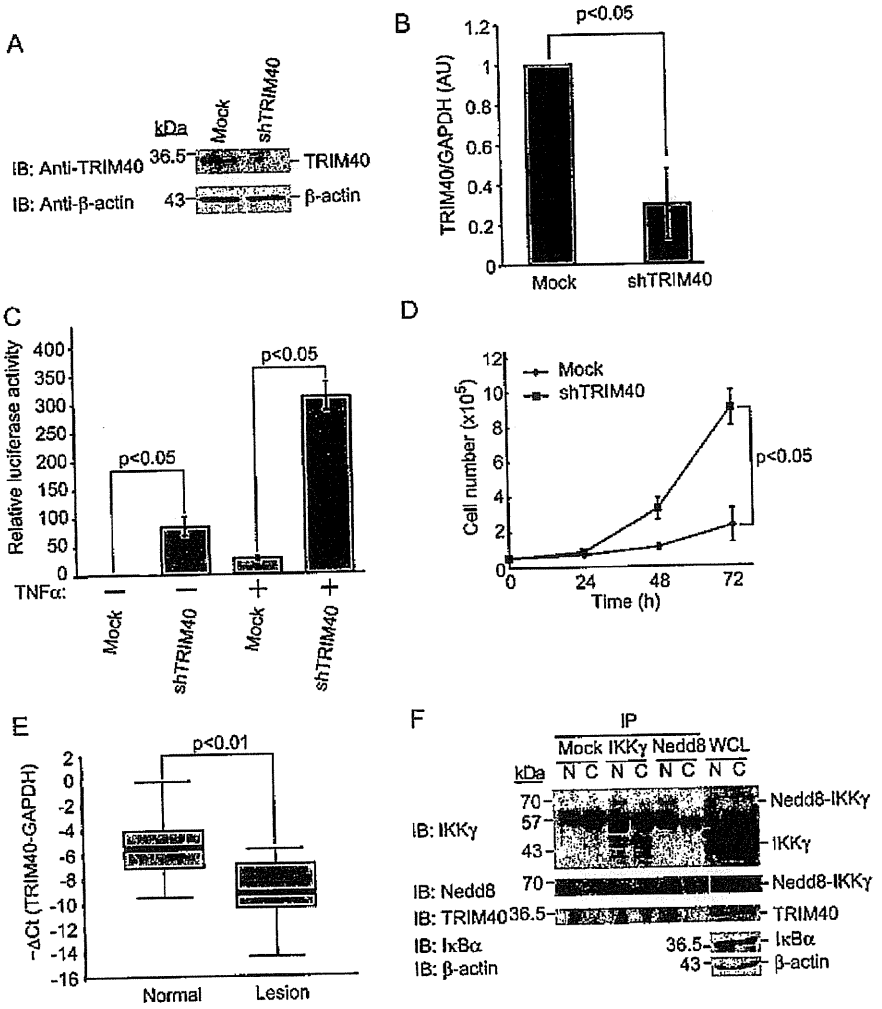

Fig. 6. Knockdown of TRIM40 promotes NF-κB-mediated transcription and accelerates cell growth. (A) Establishment of stably knocked-down IEC-6 cell lines with shRNA specific for rat *TRIM40* (shTRIM40) or with non-targeting shRNA as a control (Mock). Immunoblot analysis was performed with anti-TRIM40 or ant-β-actin antibody. (B) *TRIM40* mRNA expression in stably knocked-down IEC-6 cell lines with shRNA specific for rat *TRIM40* (shTRIM40) or with non-targeting shRNA as a control (Mock). *TRIM40* mRNA levels in these cell lines were measured by quantitative real-time PCR. (C) Knockdown of TRIM40 enhances NF-κB-mediated transcription. Stably knocked-down cells were transfected with the NF-κB luciferase reporter plasmid. Twenty-four hours after transfection, cells were treated with TNFα (20 ng/μl) and cultured for an additional 6 h and then luciferase activity was measured. Data are means ± standard deviation of values from three independent experiments. (D) Knockdown of TRIM40 causes growth delay of IEC-6 cells. Cell lines were seeded at 5×10^4 cells in six-well plates and harvested for determination of cell number at indicated times. Data are means ± standard deviation of values from three independent experiments. (E) TRIM40 is downregulated in human gastrointestinal carcinomas. *TRIM40* mRNA levels in human gastrointestinal diseases and adjacent normal tissues from 22 cases were compared by quantitative real-time PCR. The expression level of *TRIM40* mRNA was normalized to that of *GAPDH* mRNA and shown as relative expression level. The boxes within the plots represent the 25–75th percentiles. The horizontal line in the boxes indicates median value. The *P* values for the indicated comparisons were determined by Wilcoxon matched pairs test. Samples used in this assay were as follows: gastric cancers, 13; colon cancer, 3; rectal cancer, 4; benign colon tumor, 1; Crohn's disease, 1. (F) Neddylation of IKKγ in gastric cancer sample. Cell lysates were subjected to immunoprecipitation with an antibody to IKKγ or anti-Nedd8, and the resulting precipitates were subjected to immunoblot analysis with an antibody to anti-IKKγ, anti-TRIM40 or anti-Nedd8. N, normal tissues; C, cancer tissues.

knockdown of TRIM40 promoted NF-κB activity and cell growth. Taken together, these results suggest that TRIM40 is a novel-negative regulator against inflammation and carcinogenesis in the gastrointestinal tract.

It has been reported that the E3 ubiquitin ligase MDM2 promotes neddylation of p53 and negatively regulates its transcriptional activity (14) and that an F-box protein, FBXO11, which is a component of the SCF type E3 ligase, promotes neddylation of p53 and inhibits its transcriptional activity (16). Therefore, we hypothesized that TRIM40 promotes neddylation of IKKγ via a RING domain and regulates the activity of IKK complex, in which IKKγ is an essential component for activation of the canonical NF-κB pathway. Non-proteolytic lysine 63 (K63)-linked polyubiquitination has as an important role in IKK activation in the canonical NF-κB pathway (35). IKKγ specifically recognizes K63-linked polyubiquitin chains and is conjugated by K63-linked polyubiquitin chains, which induces activation of the IKK complex and promotes the NF-κB cascade (33,36,37). In addition, IKKγ is conjugated by N-terminal-linked linear polyubiquitin chains and linear polyubiquitin of IKKγ is necessary for an NF-κB pathway (34). In this study, we showed that overexpression of TRIM40 results in neddylation of IKKγ and inhibition of NF-κB activity and that knockdown of TRIM40 accelerates NF-κB activity and cell growth. Taken together, these findings indicate that non-proteolytic polyubiquitin chains by K63-linked and linear types on IKKγ positively regulate the IKK complex, whereas Nedd8 conjugation of IKKγ probably functions as a negative regulator for NF-κB activity.

Intestinal epithelial cells provide a primary physical barrier against commensal and pathogenic microorganisms in the gastrointestinal

tract, but the influence of intestinal epithelial cells on the development and regulation of immunity to infection is unknown (38). Many kinds of enterobacteria exist in the gastrointestinal tract. Despite the fact that enterobacteria are non-self antigens, the intestinal tract has no immune response for enterobacteria. The normal intestinal tract seems to have an immune suppression system for enterobacteria. In particular, chronic inflammation by pathogenic bacteria such as *H.pylori* or inflammatory bowel diseases including Crohn's disease and ulcerative colitis are closely associated with cancer (26). Evidence that has accumulated in the past decade has suggested that NF-κB plays a critical role in linking inflammation and cancer (27–30). Tissue reconstruction by chronic inflammation may induce malignant transformation of the gastrointestinal epithelium. Therefore, appropriate regulation of immune responses in the gastrointestinal tract, in which various bacteria cause inflammation, may be required for preventing carcinogenesis. We showed that TRIM40 is highly expressed in normal gastrointestinal epithelia compared with the expression level in inflammatory gastrointestinal tracts and cancer lesions. TRIM40 may downregulate production of inflammatory cytokines including TNFα, IL-6, IL-1, IL-8 via inhibition of NF-κB and prevent carcinogenesis through inflammation by enteric bacteria. Hence, TRIM40 may functions as an important regulator for maintaining homeostasis of the gastrointestinal tract.

Dysregulation of NF-κB is involved in the etiology of cancer and leukemia. Recently, NF-κB has attracted attention as a target of drugs for cancer and immune regulation. The proteasome inhibitor Bortezomib, one function of which is NF-κB inhibition through reduced IκB degradation, leading to reduced NF-κB-dependent synthesis of antiapoptotic factors, has been evaluated in a number of published and ongoing trials for solid and hematological malignancies (39). Moreover, it has been reported that the IKKβ inhibitor MLN120B inhibits TNFα-induced NF-κB activation, resulting in inhibition of the growth of multiple myeloma cell lines (40). We showed that a newly developed NF-κB inhibitor, dehydroxymethylepoxyquinomicin (DHMEQ), can be utilized for controlling allograft rejection (41). A recent study has shown that a potent and selective inhibitor of Nedd8-activating enzyme, MLN4924, disrupts cullin-RING ligase-mediated protein turnover, leading to apoptotic death in human tumor cells by dysregulation of S-phase DNA synthesis (42). Furthermore, treatment of diffuse large B-cell lymphoma cells with MLN4924 results in rapid accumulation of phosphorylated IκBα, decrease in nuclear p65 content, reduction of NF-κB transcriptional activity, and G_1 arrest, ultimately resulting in apoptosis induction. Therefore, detailed research using MLN4924 may clarify the function of TRIM40 in regulation of the NF-κB pathway. In conclusion, further functional analysis of TRIM40 may provide therapeutic benefits not only for inhibition of the growth of gastrointestinal cancers but also for the prevention of chronic inflammatory bowel diseases.

Funding

Grant-in-Aid for Scientific Research (21390087) from the Ministry of Education, Culture, Sports, Science and Technology of japan; Ono Cancer Research Fund.

Acknowledgements

The authors thank Toshio Kitamura for the plasmids, Tomoki Chiba for the antibodies, Sinya Tanaka and Takashi Saku for the cell line and Yuri Soida for help in preparing the manuscript.

Conflict of Interest Statement: None declared.

References

1 Reymond,A. *et al.* (2001) The tripartite motif family identifies cell compartments. *EMBO J.*, **20**, 2140–2151.
2 Urano,T. *et al.* (2002) Efp targets 14-3-3 sigma for proteolysis and promotes breast tumour growth. *Nature*, **417**, 871–875.
3 Gack,M.U. *et al.* (2007) TRIM25 RING-finger E3 ubiquitin ligase is essential for RIG-I-mediated antiviral activity. *Nature*, **446**, 916–920.
4 Quaderi,N.A. *et al.* (1997) Opitz G/BBB syndrome, a defect of midline development, is due to mutations in a new RING finger gene on Xp22. *Nat. Genet.*, **17**, 285–291.
5 Avela,K. *et al.* (2000) Gene encoding a new RING-B-box-Coiled-coil protein is mutated in mulibrey nanism. *Nat. Genet.*, **25**, 298–301.
6 Miyajima,N. *et al.* (2008) TRIM68 regulates ligand-dependent transcription of androgen receptor in prostate cancer cells. *Cancer Res.*, **68**, 3486–3494.
7 Kano,S. *et al.* (2008) Tripartite motif protein 32 facilitates cell growth and migration via degradation of Abl-interactor 2. *Cancer Res.*, **68**, 5572–5580.
8 Kikuchi,M. *et al.* (2009) TRIM24 mediates ligand-dependent activation of androgen receptor and is repressed by a bromodomain-containing protein, BRD7, in prostate cancer cells. *Biochim. Biophys. Acta*, **1793**, 1828–1836.
9 Kamitani,T. *et al.* (1997) Characterization of NEDD8, a developmentally down-regulated ubiquitin-like protein. *J. Biol. Chem.*, **272**, 28557–28562.
10 Lammer,D. *et al.* (1998) Modification of yeast Cdc53p by the ubiquitin-related protein rub1p affects function of the SCFCdc4 complex. *Genes Dev.*, **12**, 914–926.
11 Liakopoulos,D. *et al.* (1998) A novel protein modification pathway related to the ubiquitin system. *EMBO J.*, **17**, 2208–2214.
12 Read,M.A. *et al.* (2000) Nedd8 modification of cul-1 activates SCF(beta(TrCP))-dependent ubiquitination of IkappaBalpha. *Mol. Cell. Biol.*, **20**, 2326–2333.
13 Wu,K. *et al.* (2000) Conjugation of Nedd8 to CUL1 enhances the ability of the ROC1-CUL1 complex to promote ubiquitin polymerization. *J. Biol. Chem.*, **275**, 32317–32324.
14 Xirodimas,D.P. *et al.* (2004) Mdm2-mediated NEDD8 conjugation of p53 inhibits its transcriptional activity. *Cell*, **118**, 83–97.
15 Watson,I.R. *et al.* (2006) Mdm2-mediated NEDD8 modification of TAp73 regulates its transactivation function. *J. Biol. Chem.*, **281**, 34096–34103.
16 Abida,W.M. *et al.* (2007) FBXO11 promotes the Neddylation of p53 and inhibits its transcriptional activity. *J. Biol. Chem.*, **282**, 1797–1804.
17 Oved,S. *et al.* (2006) Conjugation to Nedd8 instigates ubiquitylation and down-regulation of activated receptor tyrosine kinases. *J. Biol. Chem.*, **281**, 21640–21651.
18 Stickle,N.H. *et al.* (2004) pVHL modification by NEDD8 is required for fibronectin matrix assembly and suppression of tumor development. *Mol. Cell. Biol.*, **24**, 3251–3261.
19 Xirodimas,D.P. *et al.* (2008) Ribosomal proteins are targets for the NEDD8 pathway. *EMBO Rep.*, **9**, 280–286.
20 Gao,F. *et al.* (2006) Neddylation of a breast cancer-associated protein recruits a class III histone deacetylase that represses NFkappaB-dependent transcription. *Nat. Cell Biol.*, **8**, 1171–1177.
21 Karin,M. *et al.* (2002) NF-kappaB in cancer: from innocent bystander to major culprit. *Nat. Rev. Cancer*, **2**, 301–310.
22 Ghosh,S. *et al.* (1990) Activation *in vitro* of NF-kappa B by phosphorylation of its inhibitor I kappa B. *Nature*, **344**, 678–682.
23 Mercurio,F. *et al.* (1997) IKK-1 and IKK-2: cytokine-activated IkappaB kinases essential for NF-kappaB activation. *Science*, **278**, 860–866.
24 Yaron,A. *et al.* (1998) Identification of the receptor component of the IkappaBalpha-ubiquitin ligase. *Nature*, **396**, 590–594.
25 Hatakeyama,S. *et al.* (1999) Ubiquitin-dependent degradation of IkappaBalpha is mediated by a ubiquitin ligase Skp1/Cul 1/F-box protein FWD1. *Proc. Natl Acad. Sci. USA*, **96**, 3859–3863.
26 Mantovani,A. *et al.* (2008) Cancer and inflammation: a complex relationship. *Cancer Lett.*, **267**, 180–181.
27 Hu,Y. *et al.* (1999) Abnormal morphogenesis but intact IKK activation in mice lacking the IKKalpha subunit of IkappaB kinase. *Science*, **284**, 316–320.
28 Pikarsky,E. *et al.* (2004) NF-kappaB functions as a tumour promoter in inflammation-associated cancer. *Nature*, **431**, 461–466.
29 Karin,M. *et al.* (2005) NF-kappaB: linking inflammation and immunity to cancer development and progression. *Nat. Rev. Immunol.*, **5**, 749–759.
30 Li,Q. *et al.* (2005) Inflammation-associated cancer: NF-kappaB is the lynchpin. *Trends Immunol.*, **26**, 318–325.
31 Okumura,F. *et al.* (2010) TRIM8 modulates STAT3 activity through negative regulation of PIAS3. *J. Cell Sci.*, **123**, 2238–2245.
32 Hayden,M.S. *et al.* (2004) Signaling to NF-kappaB. *Genes Dev.*, **18**, 2195–2224.
33 Wu,C.J. *et al.* (2006) Sensing of Lys 63-linked polyubiquitination by NEMO is a key event in NF-kappaB activation. *Nat. Cell Biol.*, **8**, 398–406.

34 Tokunaga,F. *et al.* (2009) Involvement of linear polyubiquitylation of NEMO in NF-kappaB activation. *Nat. Cell Biol.*, **11**, 123–132.
35 Chen,Z.J. *et al.* (1996) Site-specific phosphorylation of IkappaBalpha by a novel ubiquitination-dependent protein kinase activity. *Cell*, **84**, 853–862.
36 Tang,E.D. *et al.* (2003) A role for NF-kappaB essential modifier/IkappaB kinase-gamma (NEMO/IKKgamma) ubiquitination in the activation of the IkappaB kinase complex by tumor necrosis factor-alpha. *J. Biol. Chem.*, **278**, 37297–37305.
37 Ea,C.K. *et al.* (2006) Activation of IKK by TNFalpha requires site-specific ubiquitination of RIP1 and polyubiquitin binding by NEMO. *Mol. Cell*, **22**, 245–257.
38 Nagler-Anderson,C. (2001) Man the barrier! Strategic defences in the intestinal mucosa. *Nat. Rev. Immunol.*, **1**, 59–67.
39 Cusack,J.C.Jr *et al.* (2001) Enhanced chemosensitivity to CPT-11 with proteasome inhibitor PS-341: implications for systemic nuclear factor-kappaB inhibition. *Cancer Res.*, **61**, 3535–3540.
40 Hideshima,T. *et al.* (2006) MLN120B, a novel IkappaB kinase beta inhibitor, blocks multiple myeloma cell growth *in vitro* and *in vivo*. *Clin. Cancer Res.*, **12**, 5887–5894.
41 Ueki,S. *et al.* (2006) Control of allograft rejection by applying a novel nuclear factor-kappaB inhibitor, dehydroxymethylepoxyquinomicin. *Transplantation*, **82**, 1720–1727.
42 Milhollen,M.A. *et al.* (2010) MLN 4924, a NEDD8-activating enzyme inhibitor, is active in diffuse large B-cell lymphoma models: rationale for treatment of NF-kappaB-dependent lymphoma. *Blood*, **116**, 1515–1523.

Received November 29, 2010; revised March 7, 2010; accepted March 31, 2011

Cancer Science
The official journal of the Japanese Cancer Association

Inhibition of nuclear factor-kappaB suppresses peritoneal dissemination of gastric cancer by blocking cancer cell adhesion

Kazuhiro Mino,[1] Michitaka Ozaki,[2,7] Kazuaki Nakanishi,[1] Sanae Haga,[2,3] Masanori Sato,[1] Masaya Kina,[1] Masato Takahashi,[1] Norihiko Takahashi,[1] Akihiko Kataoka,[1] Kazuyoshi Yanagihara,[4] Takahiro Ochiya,[5] Toshiya Kamiyama,[1] Kazuo Umezawa[6] and Satoru Todo[1]

[1]Department of General Surgery, Graduate School of Medicine, Hokkaido University, Sapporo; [2]Department of Molecular Surgery, Hokkaido University School of Medicine, Sapporo; [3]The Japan Society for the Promotion of Science (JSPS), Tokyo; [4]Department of Life Sciences, Yasuda Women's University Faculty of Pharmacy, Hiroshima; [5]Section for Studies on Metastasis, National Cancer Center Research Institute, Tokyo; [6]Department of Applied Chemistry, Faculty of Science and Technology, Keio University, Yokohama, Japan

(Received November 4, 2010/Revised January 24, 2011/Accepted January 25, 2011/Accepted manuscript online February 2, 2011/Article first published online March 1, 2011)

Currently, patients with peritoneal dissemination of gastric cancer must accept a poor prognosis because there is no standard effective therapy. To inhibit peritoneal dissemination it is important to inhibit interactions between extracellular matrices (ECM) and cell surface integrins, which are important for cancer cell adhesion. Although nuclear factor-kappa B (NF-κB) is involved in various processes in cancer progression, its involvement in the expression of integrins has not been elucidated. We used a novel NF-κB inhibitor, dehydroxymethylepoxyquinomicin (DHMEQ), to study whether NF-κB blocks cancer cell adhesion via integrins in a gastric cancer dissemination model in mice and found that DHMEQ is a potent suppressor of cancer cell dissemination. Dehydroxymethylepoxyquinomicin suppressed the NF-κB activity of human gastric cancer cells NUGC-4 and 44As3Luc and blocked the adhesion of cancer cells to ECM when compared with the control. Dehydroxymethylepoxyquinomicin also inhibited expression of integrin (α2, α3, β1) in *in vitro* studies. In the *in vivo* model, we injected 44As3Luc cells pretreated with DHMEQ into the peritoneal cavity of mice and performed peritoneal lavage after the injection of cancer cells. Viable cancer cells in the peritoneal cavities were evaluated sequentially by *in vivo* imaging. In mice injected with DHMEQ-pretreated cells and lavaged, live cancer cells in the peritoneum were significantly reduced compared with the control, and these mice survived longer. These results indicate that DHMEQ could inhibit cancer cell adhesion to the peritoneum possibly by suppressing integrin expression. Nuclear factor-kappa B inhibition may be a new therapeutic option for suppressing postoperative cancer dissemination. (*Cancer Sci* 2011; 102: 1052–1058)

Peritoneal dissemination is the most frequent process through which gastric cancer recurs,[1] and patients with this condition must currently accept a very poor prognosis.[2,3] Standard chemotherapy is currently not sufficiently effective for improving the survival of patients with peritoneal dissemination of gastric cancer. To inhibit peritoneal dissemination, it may be important to control the adhesion of cancer cells to the peritoneum. During cancer cell dissemination in the abdominal cavity, cancer cells make contact with the basement membrane through gaps between mesothelial cells.[4,5] The basement membrane beneath mesothelial cells comprises extracellular matrices (ECM) consisting of type 1 and 4 collagen, fibronectin or laminin,[6] and mesothelial cells also produce ECM.[7] The interactions between these ECM and cell surface integrins play very important roles in cancer cell adhesion and, therefore, cancer progression.[8]

Integrins are membrane-bound proteins that form heterodimers of α- and β-subunits at the cell surface. The α-subunits vary between 120 and 180 kD, and are non-covalently associated with β-subunits (90–110 kD). To date, 14 α subunits and eight β subunits have been identified, and after mutual dimerization, these subunits contribute to cell adhesion or regulation of signal transduction required for cell survival by making contact with appropriate ECM.[9,10] It has been reported that integrins α2, α3 and β1 play important roles in the peritoneal dissemination of gastric cancer,[11] and that antibodies to these integrins suppress peritoneal dissemination of gastric cancer in a mouse model.[12]

Nuclear factor-kappaB (NF-κB) was first identified and reported in 1986[13] and studied in the context of immune and inflammatory responses.[14] Nuclear factor-kappaB is a generic term for dimers of NF-κB1 (p50/p105), NF-κB2 (p52/p100), c-Rel, RelA (p65/NF-κB3) and RelB.[15] To date, involvement of NF-κB in cancer-related molecules such as cyclin D1,[16] intercellular adhesion molecule-1 (ICAM-1), vascular cell adhesion molecule-1 (VCAM-1),[17] the Bcl family,[18] inhibitor of apoptosis (IAP), X-linked inhibitor of apoptosis protein (XIAP),[19] p53,[20] vascular endothelial growth factor (VEGF), interleukin (IL)-8,[21] MMP[22] and multidrug resistance protein 1 (MDR1),[23] has been elucidated. However, NF-κB has not been reported to be involved in cancer cell adhesion to the peritoneum via integrins.

A low-molecular-weight NF-κB inhibitor, dehydroxymethylepoxyquinomicin (DHMEQ), was newly developed by Umezawa.[24] Dehydroxymethylepoxyquinomicin specifically inhibits the nuclear translocation of p65 and prevents it binding to DNA[25]; it also has various anti-cancer effects in mouse models without obvious side-effects. Thus far, the following anti-cancer effects of DHMEQ have been reported: G1 arrest by inhibition of cyclin D1 expression;[26] and induction of apoptosis by inhibition of cIAP and XIAP,[27] or Bcl-2 and Bcl-xL.[28] Antitumor effects of DHMEQ have also been reported in *in vivo* models such as those for thyroid cancer,[27] prostate cancer,[29] hepatic cancer,[30] breast cancer,[31] pancreas cancer,[32] multiple myeloma,[28] malignant lymphoma[33] and leukemia.[26]

In the present study, we showed that NF-κB is associated with integrin expression in gastric cancer cell lines and that NF-κB inhibition by DHMEQ suppresses cancer progression by inhibiting the adhesion of gastric cancer cells to the peritoneum in a mouse model of peritoneal dissemination of gastric cancer.

[7]To whom correspondence should be addressed.
E-mail: ozaki-m@med.hokudai.ac.jp

doi: 10.1111/j.1349-7006.2011.01901.x

Materials and Methods

Cell cultures. The human gastric cancer cell line NUGC4 was obtained from the Japanese Cancer Research Resources Bank (JCRB, Osaka, Japan), and 44As3Luc with luciferase activity was constructed by one of the authors (K.Y.).[34] The 44As3Luc cells were derived from 44As3 cells, which is a highly peritoneal metastatic cell line, and were stably transfected with a pEGF-PLuc plasmid with CMV promoter (Clontech, Palo Alto, CA, USA). Human breast cancer cell lines MCF7 with constitutively low NF-κB activity and MDA-MB231 with constitutively high NF-κB activity were obtained from the American Type Culture Collection (Rockville, MD, USA).[31] The NUGC4 cells were cultured at 37°C in RPMI1640 (Sigma, St Louis, MO, USA) along with 10% fetal bovine serum (FBS); the 44As3Luc cells were cultured at the same temperature with RPMI1640 containing 100 μg/mL geneticin (Sigma); and the MCF7 and MDA-MB231 cells were also cultured at 37°C in 95% air and 5% CO_2 in DMEM (Sigma) along with 10% FBS.

Dehydroxymethylepoxyquinomycin (DHMEQ). We have originally designed and developed DHMEQ (molecular weight (MW): 261), a derivative of the natural antibiotic epoxyquinomycin C, to specifically target NF-κB.[24]

DNA-binding activity of NF-κB. To evaluate the DNA-binding activity of NF-κB in the steady state, 70% confluent cultures of NUGC4, 44As3Luc, MCF7 and MDA-MB231 in 10-cm dishes were stored at −80°C. To evaluate the effect of DHMEQ, the medium in the 70% confluent cultures of NUGC4 and 44As3Luc was replaced with 10 μg/mL DHMEQ solution, incubated for an appropriate time and stored at −80°C. The following day, nuclear proteins were extracted and examined using a p65 TransAM kit (ActiveMotif, Carlsbad, CA, USA). The absorbance was determined using a plate reader (Varioskan Flash, Thermo Fisher Scientific, Waltham, MA, USA). Each experiment was performed in triplicate.

NF-κB reporter gene assay. A GFP reporter gene construct was transfected using Cignal Reporter Assay kits (SA Biosciences, Frederick, MD, USA). Cultured cells were trypsinized and resuspended in Opti-MEM (Invitrogen, Carlsbad, CA, USA) with non-essential amino acids (Invitrogen) without antibiotics at a concentration of 2×10^5 cells in a 96-well plate. Cells were transfected with the reporter by culturing for 16 h with Surefect (SA Biosciences). After the medium was replaced with Opti-MEM with penicillin/streptomycin, the cells were incubated for an additional 8 h. The medium was then replaced with Opti-MEM containing 10 μg/mL of DHMEQ (or 0.024% of DMSO for the controls). The intensity of fluorescence was measured at appropriate times in triplicate using Varioskan Flash (excitation, 470 nm; emission, 515 nm).

mRNA expression of integrins in DHMEQ-treated cells. Real-time PCR was used to examine mRNA expression. The 44As3Luc cells were cultured in triplicate in 0.024% DMSO solution (controls) or in 10 μg/mL DHMEQ for the appropriate times. Total RNA was isolated using an RNeasy mini kit (Qiagen, Valencia, CA, USA) in accordance with the manufacturer's instructions. For cDNA synthesis, ReverTra Ace qPCR RT kit (Toyobo, Osaka, Japan) with Oligo(dT) 20 primer (Toyobo) was used in accordance with the manufacturer's instructions. For relative quantification by PCR, each cDNA product was analyzed in a LightCycler (version 1.4) using a QuantiTect SYBR Green PCR kit (Qiagen).

Flow cytometric analysis of integrin expression. p65 silencing was performed using p65 siRNA2 (BD Biosciences, Bedford, MA, USA). Next, 50% confluent cells were incubated for 24 h in medium without antibiotics in 10-cm dishes. Then, 33 nM p65 siRNA was added to each dish and transfected for 48 h. p65 silencing was confirmed by western blot analysis using primary antibodies against ×500 α-tubulin and ×1000 p65 protein (Cell Signaling, Beverly, MA, USA) and ×5000 goat anti-mouse IgG for tubulin or anti-rabbit IgG for the p65 protein. With regard to DHMEQ treatment, the medium in 70% confluent cell cultures in 10-cm dishes was replaced with 10 μg/mL DHMEQ solution (0.024% DMSO for the controls) and cultured for the appropriate times. These cells were trypsinized and analyzed using flow cytometry (FACS Caliber; Becton Dickinson, Franklin Lakes, NJ, USA). The antibodies used for these assays were integrin α2, integrin α3, integrin β1 and isotype controls for these integrins. All antibodies were obtained from R&D Systems (Minneapolis, MN, USA).

Adhesion assay. We evaluated the anti-adhesive effect of DHMEQ by using a plate pre-coated with ECM constituting the peritoneal basement membrane. The medium in 70% confluent cell cultures in 10-cm dishes was replaced with 10 μg/mL DHMEQ solution (or 0.024% DMSO for the controls), and the dishes were incubated for 24 h. These cells were trypsinized, assembled, adjusted to a concentration of 1×10^6 cells/mL with RPMI and distributed on the pre-coated plates (80 μL per plate). Next, the cells were incubated at 37°C for 1 h. Except for the non-treated plate, all plates were washed three times with 100 μL of FBS-free RPMI. After washing, 10 μL of ×50 diluted Cell Counting kit F (CCKF; Dojindo, Osaka, Japan) was added to each well, and the fluorescence intensity of the remaining live cells (adhesive cells) was evaluated using Varioskan Flash at 30 min after CCKF administration (excitation, 490 nm; emission, 515 nm). Pre-coated plates were manufactured by BD Biosciences and the ECM coated on the plates were types 1 and 4 collagen, fibronectin and laminin.

DHMEQ cytotoxicity assay. The cells were seeded into 96-well plates at 5×10^3 cells/well in 10% FBS-containing medium. Twenty-four hours later, the medium in the wells was replaced with different concentrations of DHMEQ solution or 0.048% DMSO solution, and the cells were then incubated again for 24 h. Lactate dehydrogenase (LDH) activity of the supernatant was measured using an LDH cytotoxicity detection kit (Takara Bio, Shiga, Japan).

Animal experiments. Six-week-old male BALB/c-nu/nu mice, each weighing approximately 20 g, were obtained from CLEA Japan, Inc. (Tokyo, Japan). The mice were grouped as follows: (i), implantation of DMSO-treated cells; (ii) implantation of DHMEQ-treated cells; (iii) implantation of DMSO-treated cells with peritoneal lavage; and (iv) implantation of DHMEQ-treated cells with peritoneal lavage. Each group comprised four mice. Then, 2×10^6 44As3Luc cells, which had been treated with 10 μg/mL DHMEQ (or 0.024% DMSO for the controls) for 24 h, were injected intraperitoneally into the above mentioned mice. One hour after injection, laparotomy and peritoneal lavage were performed using phosphate-buffered saline (PBS). Peritoneal lavage was performed through a 1-cm incision through which 5 mL of PBS was slowly injected. Bio-imaging was performed before and after the peritoneal lavage, and on days 2, 5, 10, 15 and 20 in order to evaluate cancer progression. Luminescence was evaluated at approximately 7 min after intraperitoneal injection of 1500 μg/mouse D-luciferin potassium salt (Synchem OHG, Altenburg, Germany). *In vivo* imaging was performed using Photon Imager Hu (Biospace Lab, Paris, France) with the mice under isoflurane anesthesia (Abbott Japan, Tokyo, Japan). Images were captured using Photo Acquisition 2.6 (Biospace Lab) with 0.5 min exposure and processed using Photo Vision Plus. Signal intensity was quantified as the sum of all detected photon counts (count per minute [CPM]) within the region of interest (ROI). All procedures involving animals and their care were approved by the Ethics Committee of Hokkaido University in accordance with institutional and Japanese governmental guidelines for animal experiments.

Scanning electron microscopy (SEM) of the peritoneal wall. The peritoneal walls of mice injected with cancer cells

were fixed with 10% formaldehyde for 180 min and then overnight at 4°C with 1.25% glutaraldehyde solution. The fixed samples were dehydrated in a 30–100% graded ethanol series and immersed in tert-butyl alcohol overnight at −20°C. These samples were dried using ES-2000 (Hitachi High-Technologies Co., Tokyo, Japan) for 3 h and ion-sputtered using E-1030 (Hitachi) for 120 s. The peritoneal surface was observed under a scanning electron microscope (S-3500N; Hitachi).

Statistics. The mean and SD were calculated for all variables, except the data from the flow cytometry. Between-group statistical significance was determined using the Student's *t* test. $P < 0.05$ was considered as statistically significant.

Results

DHMEQ effectively suppresses p65-DNA binding activity in gastric cancer cells. In the steady state, the p65-DNA binding activities in NUGC4 and 44As3Luc cells were as high as that in MDA-MB231 cells, a positive control cell with high binding activity. The activity in MCF7 cells is constitutively low as previously reported [31], and hence these cells were used as the negative control (Fig. 1A). The binding activities in both cells reached their lowest levels 2 h after the addition of 10 μg/mL DHMEQ (as a final concentration) and returned to initial conditions within 24 h (Fig. 1B). A GFP reporter assay showed that DHMEQ significantly suppresses transcriptional activity in both cells (Fig. 1C). On the basis of these results, we considered that DHMEQ had a similar effect in NUGC4 and 44As3Luc cells. Therefore, we used 44As3Luc cells in the following experiments. We planned to evaluate cancer progression using bioimaging.

Effect of NF-κB inhibition on integrin expression. In 44As3Luc cells, the mRNA of all integrins – α2, α3 and β1 – were significantly suppressed 2 h after the addition of 10 μg/mL DHMEQ (as a final concentration) compared with the control to which DMSO was added (Fig. 2A). The percentage reduction in the expressions of integrins α2, α3 and β1 was 27%, 31% and 8%, respectively. Flow cytometric analysis revealed that the expressions of all cell surface integrins on 44As3Luc cells were gradually suppressed after the addition of DHMEQ (Fig. 2B). Reductions in integrin expression (α2, α3 and β1) following DHMEQ addition was 68%, 83% and 45% at 24 h, respectively. Similarly, flow cytometric analysis of integrins α2, α3 and β1 revealed that the expressions of cell surface integrins in p65-deleted cells were suppressed to the same degree as in DHMEQ-treated cells (Fig. 2C). Reductions in integrin expression after p65 deletion were 34% (α2), 76% (α3) and 41% (β1). p65 silencing was confirmed by western blotting for nuclear and cytoplasmic p65 proteins (Fig. 2D).

Anti-adhesive effect of DHMEQ-treated cells in an *in vitro* assay. Significantly fewer 44As3Luc cells treated with 10 μg/mL DHMEQ (final concentration) remained alive on plates pre-coated with ECM after they were washed (ECM-adhesive cells) than 44As3Luc cells treated with DMSO (Fig. 3A). Reductions in the numbers of adhesive cells following DHMEQ addition were 18.3% (laminin), 34.8% (fibronectin), 38.2% (type 1 collagen) and 43.5% (type 4 collagen). The LDH value, which represents the cytotoxic effect, was significantly elevated in the supernatant of cells treated with DHMEQ at concentrations >17.5 μg/mL (Fig. 3B).

Effect of peritoneal lavage on implantation of DHMEQ-treated cancer cells on the abdominal wall. The number of cancer cells decreased in mice injected with DHMEQ-pretreated cells and subjected to peritoneal lavage (Fig. 4A). The intensity of bioluminescence after lavage was significantly reduced (reduction rate, 39%) in mice that were injected with DHMEQ-pretreated cells and subjected to peritoneal lavage compared with in mice injected with DMSO-pretreated control cells and subjected to

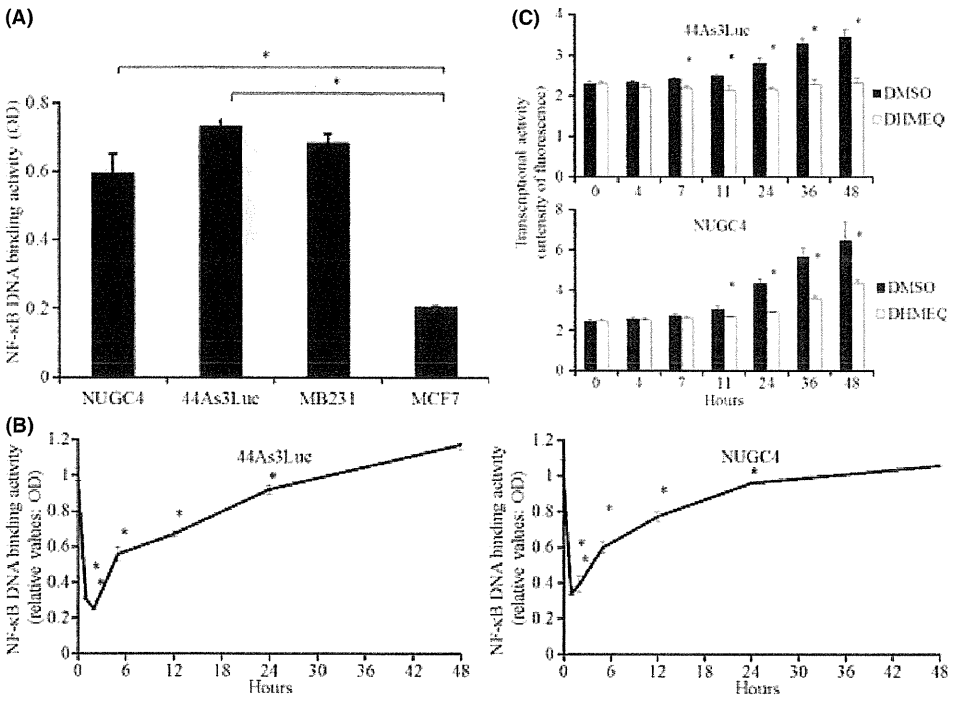

Fig. 1. Dehydroxymethylepoxyquinomicin (DHMEQ) effectively suppressed p65-DNA binding activity in gastric cancer cells. (A) Nuclear p65 protein binding activity to DNA in a steady state. MDA-MB231 cells were used as a positive control, and MCF7 cells were used as a negative one. *$P < 0.05$. (B) Time course of binding activity of nuclear p65 proteins to DNA in DHMEQ-treated cells. The binding activities of both cells were assessed at 2, 6, 12, 24 and 48 h after DHMEQ administration. *Significantly <0 h ($P < 0.05$). (C) Nuclear factor-kappa B (NF-κB) GFP reporter assay. The black bars show cells treated with DMSO, and white bars show those with DHMEQ. *Significantly more than controls ($P < 0.05$). OD, optical density.

doi: 10.1111/j.1349-7006.2011.01901.x

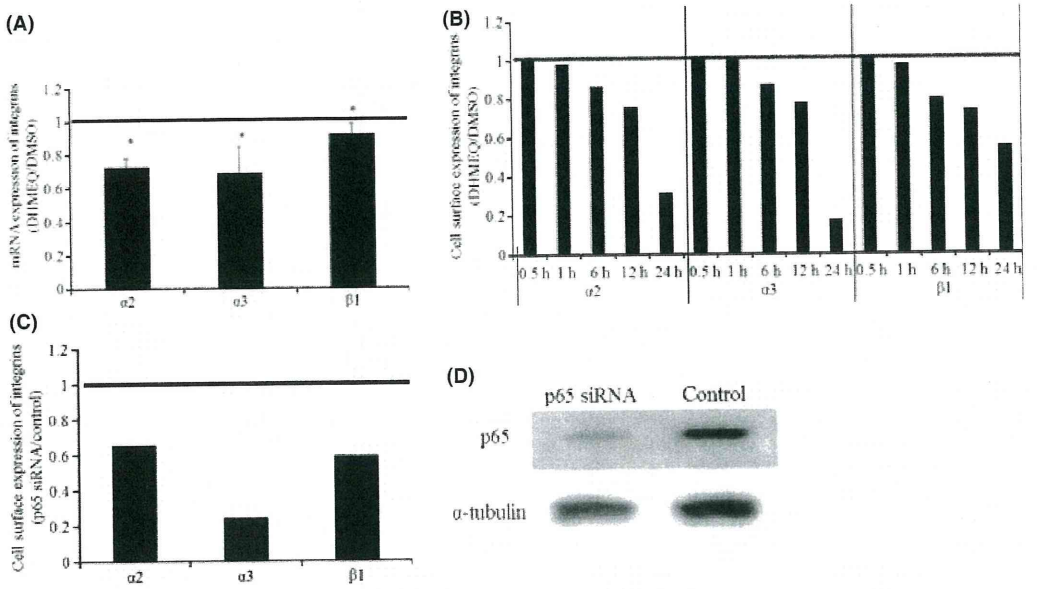

Fig. 2. Effect of nuclear factor-kappa B (NF-κB) inhibition on expression of adhesion molecules. (A) Quantitative evaluation of mRNA of integrins by real-time PCR. The graph shows the average of the ratio of copies of dehydroxymethylepoxyquinomicin (DHMEQ)-treated 44As3Luc cells to DMSO-treated cells at 2 h after DHMEQ administration. When the longitudinal value is below 1 (bold line), the integrin expression of DHMEQ-treated cells is lower than that of DMSO-treated cells. *Significantly less than controls ($P < 0.05$). (B) Expression of cell surface integrins of DHMEQ-treated cells. The graph shows the expression rate of cell surface adhesion molecules of 44As3Luc cells treated with DHMEQ compared with that of DMSO-treated cells for each time point. The bold line is as described above. (C) Expression of cell surface adhesion molecules of cells knocked down by p65 siRNA. The graph shows the rate of cell surface integrins of 44As3Luc cells knocked down by p65 siRNA. The bold line is as described above. (D) p65 deletion. The p65 deletion was confirmed by western blotting.

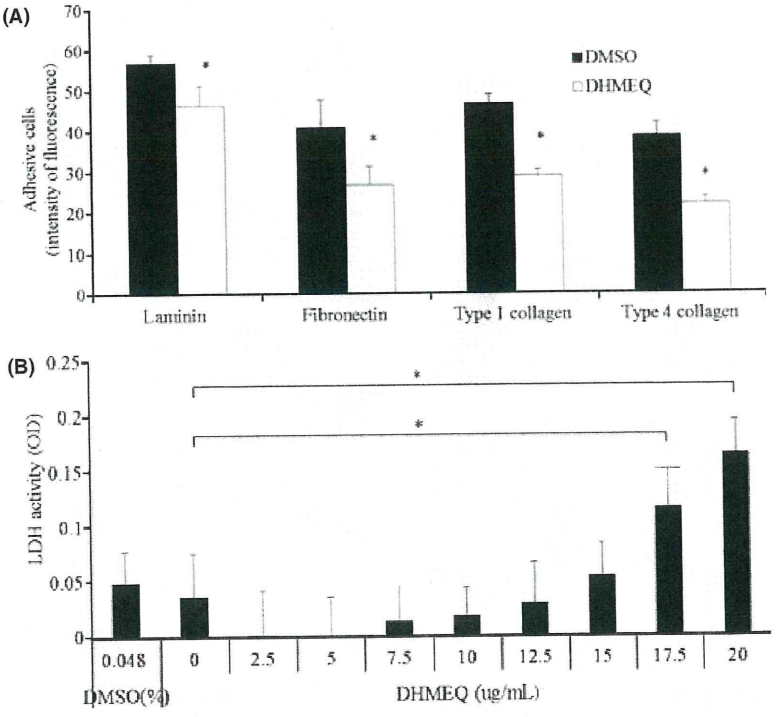

Fig. 3. Anti-adhesive effect of dehydroxymethylepoxyquinomicin (DHMEQ) pretreated cells in the *in vitro* study. (A) Adhesion assay. The bars show the fluorescence intensity of the remaining live cells on the plates. The black bars show cells pretreated with DHMEQ, and white bars show those with DMSO. *Significantly less than controls ($P < 0.05$). (B) Evaluation of cytotoxicity of DHMEQ. The graph shows lactate dehydrogenase (LDH) activity of the supernatant of the 44As3Luc cells treated with DHMEQ or DMSO. *$P < 0.05$. OD, optical density.

peritoneal lavage (Fig. 4B). The SEM revealed that cancer cells adhered less to the basement membrane of the peritoneum in mice injected with DHMEQ-pretreated cells than in those injected with DMSO-pretreated control cells (Fig. 4C).

Follow up of gastric cancer dissemination by *in vivo* imaging. The DHMEQ-pretreated 44As3Luc cells injected in mice grew slowly compared with the DMSO-pretreated cells (Fig. 5A). The increase in the CPM/mm^2 value of the

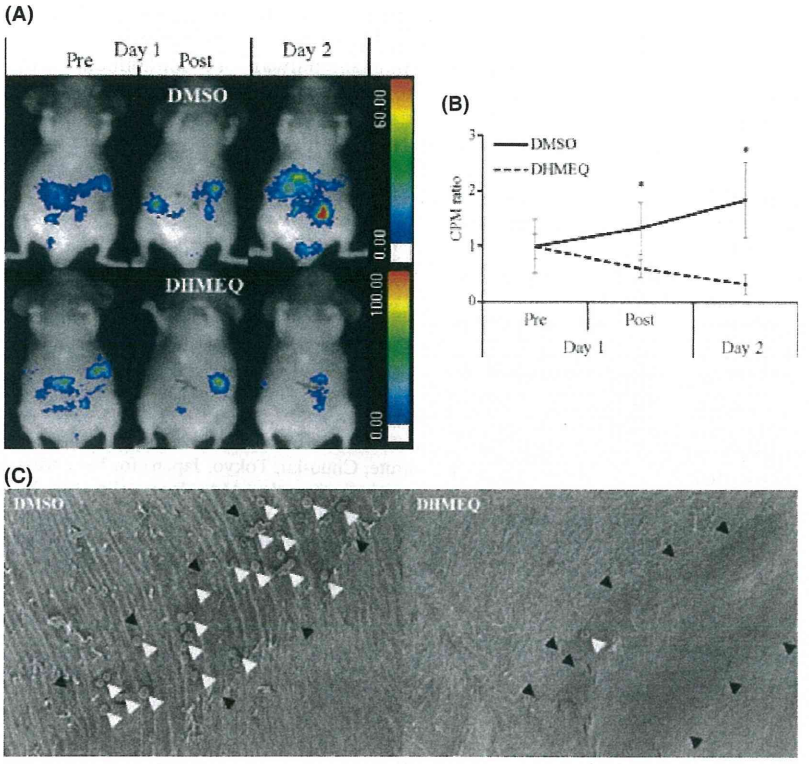

Fig. 4. Peritoneal lavage inhibited cancer cells pretreated with dehydroxymethylepoxyquinomicin (DHMEQ) from implanting into the abdominal wall. (A) *In vivo* imaging at around the time of peritoneal lavage. The luminescent value indicates the number of live cells in the abdominal wall. Pre/Post means before/after the peritoneal lavage. (B) Count per minute (CPM)/mm^2 value of pre/post peritoneal lavage. The graph shows the time course of the CPM/mm^2 value compared with the time of cancer cell injection. Initial values were adjusted to 1. *Significantly less than controls ($P < 0.05$). (C) SEM findings of the peritoneum. Left: abdominal wall injected with 44As3Luc cells pretreated with DHMEQ. Right: those with DMSO. The area indicated by black arrowheads is the area exposed to the peritoneal cavity. White arrowheads show the adhesive cancer cells.

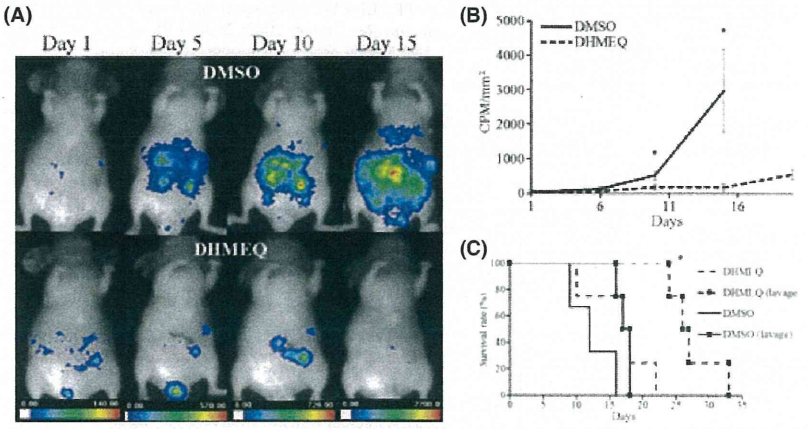

Fig. 5. Follow up after peritoneal lavage. (A) Follow-up imaging of mice subjected to peritoneal lavage. The range bars were adjusted for mice injected with DMSO pretreated cells at every evaluation day. (B) Time course of the count per minute (CPM)/mm^2 value. The black line represents the mice that were injected with DMSO-pretreated cells, and the broken line represents those injected with dehydroxymethylepoxyquinomicin (DHMEQ)-pretreated cells. *Significantly less than controls ($P < 0.05$). (C) Kaplan–Meier analysis of the survival of all groups. The line is as described above. The line with markers represents mice subjected to peritoneal lavage. *Significantly prolonged than all other groups ($P < 0.05$).

DHMEQ-treated cells was significantly delayed. The error bar of the CPM/mm^2 value of the DMSO-pretreated group ranged widely, because malignant ascites possibly obscured luminescent emission at the terminal stage (Fig. 5B). Survival was only significantly prolonged in mice injected with DHMEQ-treated cells and subjected to peritoneal lavage (Fig. 5C).

Discussion

NF-κB is undoubtedly involved in various biological properties of cancer cells.[35] However, its involvement in the expression of integrins, which are associated with cancer cell adhesion to the peritoneum, has not been reported. In the present study, we investigated whether NF-κB is involved in cell adhesion to the peritoneum via regulation of integrin expression, and whether DHMEQ, as a novel NF-κB inhibitor, suppresses the dissemination of gastric cancer in a mouse model.

Several investigators reported that NF-κB activity is associated with peritoneal dissemination of cancer cells.[36–38] Sasaki *et al.*[39] evaluated human gastric cancer tissues by immunohistochemical analysis, where NF-κB activation was significantly correlated with peritoneal metastases and survival. Our results in the present study support the previously reported data that NF-κB activity of gastric cancer cell lines was markedly activated and with highly metastatic behavior, and that DHMEQ sufficiently inhibited NF-κB activity and eventually suppressed the peritoneal dissemination.

Integrins are also associated with malignant potential.[40–42] Integrins play an important role in cancer cell adhesion to the peritoneum by enabling contact with appropriate ECM. Oosterling *et al.*[43] showed that anti-β1 integrin antibody reduces surgery-induced adhesion of colon carcinoma cells to traumatized peritoneal surfaces. Fishman *et al.*[44] showed similar findings using ovarian cancer cell lines in the *in vitro* analysis. With

doi: 10.1111/j.1349-7006.2011.01901.x

regard to gastric cancer, integrins α2, α3 and β1 are key molecules in animal models and humans.[11,12,45,46] The ligands of integrin α2β1 are collagens and laminin, and those of α3β1 are fibronectin, laminin,and collagens.[10] In our *in vitro* study, DHMEQ suppressed cancer cell adhesion to the peritoneum via p65-mediated suppression of integrin expression. Also, Takatsuki *et al.*[12] reported that anti-α3 antibody strongly suppressed the adhesion of gastric cancer cells to mice peritoneum. This integrin α3 was suppressed most by DHMEQ in this study. Therefore, DHMEQ may suppress cancer cell adhesion mainly via integrin α3, while DHMEQ may associate with other adhesion molecules that are not examined in this study.

In our *in vivo* study, viable cells in mice injected with DHMEQ-treated cells and subjected to peritoneal lavage still decreased on day 2 and only this group survived significantly longer. This finding might suggest that DHMEQ exerts another effect via the anti-adhesive effect. Jiang *et al.*[47] reported that NF-κB inhibition by IκBβ reduces anchorage-independent growth in a lung cancer cell line. Scaife *et al.*[48] showed that NF-κB inhibitor causes anoikis in a human colon cancer cell line. It might be possible that DHMEQ is associated with a pro-anoikis effect in gastric cancer dissemination.

In the present study, we first demonstrated that NF-κB could play a pivotal role in the progression of gastric cancer via the regulation of integrin expression and promotion of adhesion of cancer cells to the peritoneal wall. In our *in vivo* study, a specific deletion of NF-κB (p65) by siRNA was not performed, because we considered that transient deletion of p65 protein does not reflect the same result of DHMEQ-administered cells. Additionally, we could not clarify whether the DHMEQ effect on integrins is unique to the integrin pathway or concomitant with other phenomenon such as apoptosis. Further studies are required to clarify the involvement of integrins or other molecules in the anti-adhesive effect of DHMEQ against cancer cells. We believe that NF-κB inhibitors such as DHMEQ may be potential therapeutic options to prevent gastric cancer progression during peri-operative periods.

Acknowledgments

This study were supported by the Program for Promotion of Fundamental Studies in Health Sciences of the National Institute of Biomedical Innovation (NIBIO) and by a Grant-in-Aid for Scientific Research from the Ministry of Education, Culture, Sports, Science and Technology of Japan (#17390357 and #19659317 to M.O., # 21390369 to T.K.). We also thank Dr M. Takigahira (Section for Studies on Metastasis, National Cancer Center Research Institute, Chuo-ku, Tokyo, Japan) for her excellent technical support for constructing the 44As3Luc cells, Ms N. Kobayashi (Department of General Surgery, Graduate School of Medicine, Hokkaido University, Sapporo, Japan) for performing the real-time PCR assay and Dr H. Maeda (Creative Research Institution, Hokkaido University, Sapporo, Japan) for processing the samples for SEM.

Disclosure Statement

The authors have no conflict of interest.

References

1 Sasako M. Principles of surgical treatment for curable gastric cancer. *J Clin Oncol* 2003; **21**: 274s–5s.
2 Schott A, Vogel I, Krueger U *et al.* Isolated tumor cells are frequently detectable in the peritoneal cavity of gastric and colorectal cancer patients and serve as a new prognostic marker. *Ann Surg* 1998; **227**: 372–9.
3 Sadeghi B, Arvieux C, Glehen O *et al.* Peritoneal carcinomatosis from non-gynecologic malignancies: results of the EVOCAPE 1 multicentric prospective study. *Cancer* 2000; **88**: 358–63.
4 Kimura A, Koga S, Kudoh H, Iitsuka Y. Peritoneal mesothelial cell injury factors in rat cancerous ascites. *Cancer Res* 1985; **45**: 4330–3.
5 Yonemura Y, Endo Y, Obata T, Sasaki T. Recent advances in the treatment of peritoneal dissemination of gastrointestinal cancers by nucleoside antimetabolites. *Cancer Sci* 2007; **98**: 11–8.
6 Witz CA, Montoya-Rodriguez IA, Cho S, Centonze VE, Bonewald LF, Schenken RS. Composition of the extracellular matrix of the peritoneum. *J Soc Gynecol Investig* 2001; **8**: 299–304.
7 Lessan K, Aguiar DJ, Oegema T, Siebenson L, Skubitz AP. CD44 and beta1 integrin mediate ovarian carcinoma cell adhesion to peritoneal mesothelial cells. *Am J Pathol* 1999; **154**: 1525–37.
8 Ruoslahti E, Giancotti FG. Integrins and tumor cell dissemination. *Cancer Cells* 1989; **1**: 119–26.
9 Hehlgans S, Haase M, Cordes N. Signalling via integrins: implications for cell survival and anticancer strategies. *Biochim Biophys Acta* 2007; **1775**: 163–80.
10 Hynes RO. Integrins: versatility, modulation, and signaling in cell adhesion. *Cell* 1992; **69**: 11–25.
11 Nishimura S, Chung YS, Yashiro M, Inoue T, Sowa M. Role of alpha 2 beta 1- and alpha 3 beta 1-integrin in the peritoneal implantation of scirrhous gastric carcinoma. *Br J Cancer* 1996; **74**: 1406–12.
12 Takatsuki H, Komatsu S, Sano R, Takada Y, Tsuji T. Adhesion of gastric carcinoma cells to peritoneum mediated by alpha3beta1 integrin (VLA-3). *Cancer Res* 2004; **64**: 6065–70.
13 Sen R, Baltimore D. Multiple nuclear factors interact with the immunoglobulin enhancer sequences. *Cell* 1986; **46**: 705–16.
14 Berkholtz CB, Lai BE, Woodruff TK, Shea LD. Distribution of extracellular matrix proteins type I collagen, type IV collagen, fibronectin, and laminin in mouse folliculogenesis. *Histochem Cell Biol* 2006; **126**: 583–92.
15 Verma IM, Stevenson JK, Schwarz EM, Van Antwerp D, Miyamoto S. Rel/NF-kappa B/I kappa B family: intimate tales of association and dissociation. *Genes Dev* 1995; **9**: 2723–35.
16 Donnellan R, Chetty R. Cyclin D1 and human neoplasia. *Mol Pathol* 1998; **51**: 1–7.
17 Bonizzi G, Karin M. The two NF-kappaB activation pathways and their role in innate and adaptive immunity. *Trends Immunol* 2004; **25**: 280–8.
18 Karin M, Cao Y, Greten FR, Li ZW. NF-kappaB in cancer: from innocent bystander to major culprit. *Nat Rev Cancer* 2002; **2**: 301–10.
19 Deveraux QL, Reed JC. IAP family proteins – suppressors of apoptosis. *Genes Dev* 1999; **13**: 239–52.
20 Tergaonkar V, Pando M, Vafa O, Wahl G, Verma I. p53 stabilization is decreased upon NFkappaB activation: a role for NFkappaB in acquisition of resistance to chemotherapy. *Cancer Cell* 2002; **1**: 493–503.
21 Huang S, Robinson JB, Deguzman A, Bucana CD, Fidler IJ. Blockade of nuclear factor-kappaB signaling inhibits angiogenesis and tumorigenicity of human ovarian cancer cells by suppressing expression of vascular endothelial growth factor and interleukin 8. *Cancer Res* 2000; **60**: 5334–9.
22 Rangaswami H, Bulbule A, Kundu GC. Nuclear factor-inducing kinase plays a crucial role in osteopontin-induced MAPK/IkappaBalpha kinase-dependent nuclear factor kappaB-mediated promatrix metalloproteinase-9 activation. *J Biol Chem* 2004; **279**: 38921–35.
23 Bentires-Alj M, Barbu V, Fillet M *et al.* NF-kappaB transcription factor induces drug resistance through MDR1 expression in cancer cells. *Oncogene* 2003; **22**: 90–7.
24 Ariga A, Namekawa J, Matsumoto N, Inoue J, Umezawa K. Inhibition of tumor necrosis factor-alpha-induced nuclear translocation and activation of NF-kappa B by dehydroxymethylepoxyquinomicin. *J Biol Chem* 2002; **277**: 24625–30.
25 Yamamoto M, Horie R, Takeiri M, Kozawa I, Umezawa K. Inactivation of NF-kappaB Components by Covalent Binding of (−)-Dehydroxymethylepoxyquinomicin to Specific Cysteine Residues. *J Med Chem* 2008; **51**: 5780–8.
26 Watanabe M, Ohsugi T, Shoda M *et al.* Dual targeting of transformed and untransformed HTLV-1-infected T cells by DHMEQ, a potent and selective inhibitor of NF-kappaB, as a strategy for chemoprevention and therapy of adult T-cell leukemia. *Blood* 2005; **106**: 2462–71.
27 Starenki DV, Namba H, Saenko VA *et al.* Induction of thyroid cancer cell apoptosis by a novel nuclear factor kappaB inhibitor, dehydroxymethylepoxyquinomicin. *Clin Cancer Res* 2004; **10**: 6821–9.
28 Tatetsu H, Okuno Y, Nakamura M *et al.* Dehydroxymethylepoxyquinomicin, a novel nuclear factor-kappaB inhibitor, induces apoptosis in multiple myeloma cells in an IkappaBalpha-independent manner. *Mol Cancer Ther* 2005; **4**: 1114–20.
29 Kikuchi E, Horiguchi Y, Nakashima J *et al.* Suppression of hormone-refractory prostate cancer by a novel nuclear factor kappaB inhibitor in nude mice. *Cancer Res* 2003; **63**: 107–10.
30 Nishimura D, Ishikawa H, Matsumoto K *et al.* DHMEQ, a novel NF-kappaB inhibitor, induces apoptosis and cell-cycle arrest in human hepatoma cells. *Int J Oncol* 2006; **29**: 713–9.

31 Matsumoto G, Namekawa J, Muta M *et al.* Targeting of nuclear factor kappaB Pathways by dehydroxymethylepoxyquinomicin, a novel inhibitor of breast carcinomas: antitumor and antiangiogenic potential in vivo. *Clin Cancer Res* 2005; **11**: 1287–93.
32 Matsumoto G, Muta M, Umezawa K *et al.* Enhancement of the caspase-independent apoptotic sensitivity of pancreatic cancer cells by DHMEQ, an NF-kappaB inhibitor. *Int J Oncol* 2005; **27**: 1247–55.
33 Dabaghmanesh N, Matsubara A, Miyake A *et al.* Transient inhibition of NF-kappaB by DHMEQ induces cell death of primary effusion lymphoma without HHV-8 reactivation. *Cancer Sci* 2009; **100**: 737–46.
34 Yanagihara K, Takigahira M, Takeshita F *et al.* A photon counting technique for quantitatively evaluating progression of peritoneal tumor dissemination. *Cancer Res* 2006; **66**: 7532–9.
35 Nakanishi C, Toi M. Nuclear factor-kappaB inhibitors as sensitizers to anticancer drugs. *Nat Rev Cancer* 2005; **5**: 297–309.
36 Mabuchi S, Ohmichi M, Nishio Y *et al.* Inhibition of inhibitor of nuclear factor-kappaB phosphorylation increases the efficacy of paclitaxel in in vitro and in vivo ovarian cancer models. *Clin Cancer Res* 2004; **10**: 7645–54.
37 Nakahara C, Nakamura K, Yamanaka N *et al.* Cyclosporin-A enhances docetaxel-induced apoptosis through inhibition of nuclear factor-kappaB activation in human gastric carcinoma cells. *Clin Cancer Res* 2003; **9**: 5409–16.
38 Shao M, Cao L, Shen C *et al.* Epithelial-to-mesenchymal transition and ovarian tumor progression induced by tissue transglutaminase. *Cancer Res* 2009; **69**: 9192–201.
39 Sasaki N, Morisaki T, Hashizume K *et al.* Nuclear factor-kappaB p65 (RelA) transcription factor is constitutively activated in human gastric carcinoma tissue. *Clin Cancer Res* 2001; **7**: 4136–42.
40 Pontes-Junior J, Reis ST, de Oliveira LC *et al.* Association between integrin expression and prognosis in localized prostate cancer. *Prostate* 2010; **70**: 1189–95.
41 Dingemans AM, van den Boogaart V, Vosse BA, van Suylen RJ, Griffioen AW, Thijssen VL. Integrin expression profiling identifies integrin alpha5 and beta1 as prognostic factors in early stage non-small cell lung cancer. *Mol Cancer* 2010; **9**: 152.
42 Takayama N, Arima S, Haraoka S, Kotho T, Futami K, Iwashita A. Relationship between the expression of adhesion molecules in primary esophageal squamous cell carcinoma and metastatic lymph nodes. *Anticancer Res* 2003; **23**: 4435–42.
43 Oosterling SJ, van der Bij GJ, Bogels M *et al.* Anti-beta1 integrin antibody reduces surgery-induced adhesion of colon carcinoma cells to traumatized peritoneal surfaces. *Ann Surg* 2008; **247**: 85–94.
44 Fishman DA, Kearns A, Chilukuri K *et al.* Metastatic dissemination of human ovarian epithelial carcinoma is promoted by alpha2beta1-integrin-mediated interaction with type I collagen. *Invasion Metastasis* 1998; **18**: 15–26.
45 Kawamura T, Endo Y, Yonemura Y *et al.* Significance of integrin alpha2/beta1 in peritoneal dissemination of a human gastric cancer xenograft model. *Int J Oncol* 2001; **18**: 809–15.
46 Matsuoka T, Yashiro M, Nishimura S *et al.* Increased expression of alpha2beta1-integrin in the peritoneal dissemination of human gastric carcinoma. *Int J Mol Med* 2000; **5**: 21–5.
47 Jiang Y, Cui L, Yie TA, Rom WN, Cheng H, Tchou-Wong KM. Inhibition of anchorage-independent growth and lung metastasis of A549 lung carcinoma cells by IkappaBbeta. *Oncogene* 2001; **20**: 2254–63.
48 Scaife CL, Kuang J, Wills JC *et al.* Nuclear factor kappaB inhibitors induce adhesion-dependent colon cancer apoptosis: implications for metastasis. *Cancer Res* 2002; **62**: 6870–8.

doi: 10.1111/j.1349-7006.2011.01901.x